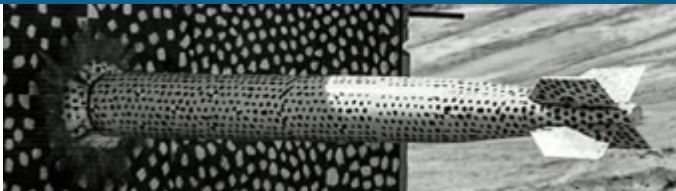
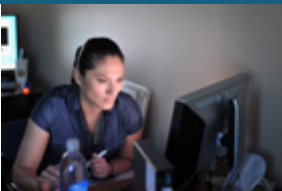




# Data-driven plastic anisotropy predictions using crystal plasticity and deep learning models

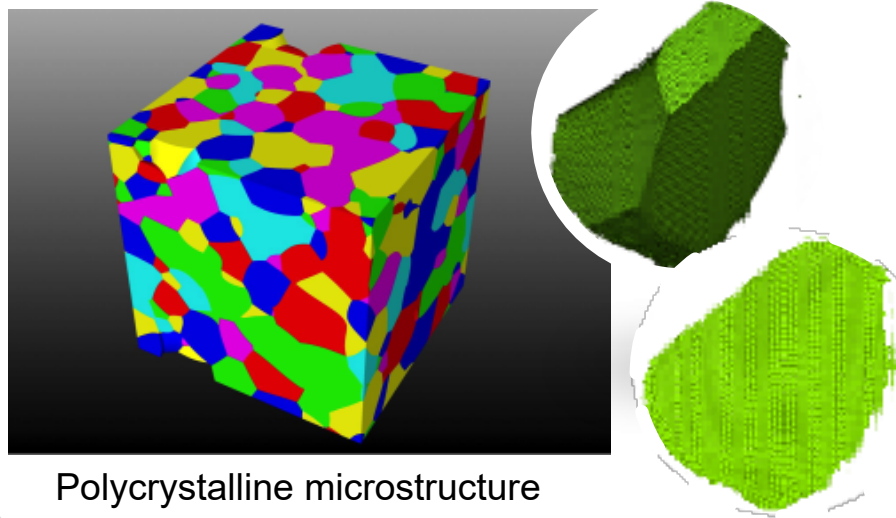


*David Montes de Oca Zapiain<sup>1</sup>, Hojun Lim<sup>1</sup>,  
Taejoon Park<sup>2</sup>, Farhang Pourboghrat<sup>2</sup>*

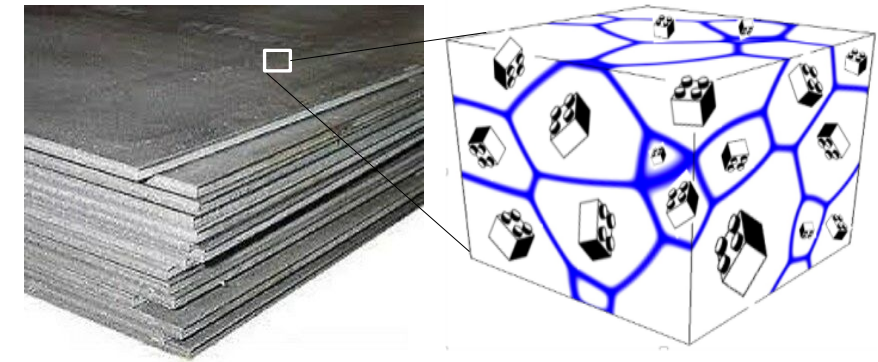
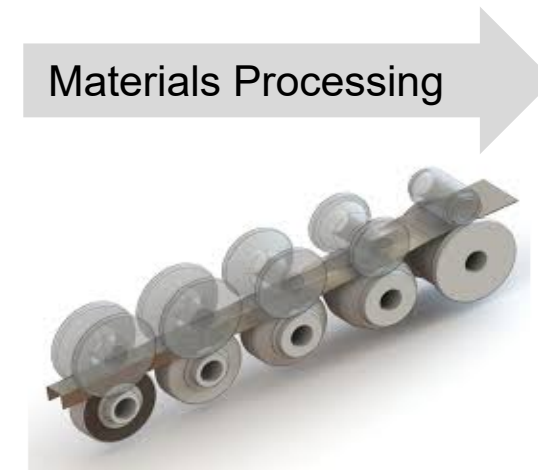


<sup>1</sup>*Sandia National Laboratories*  
<sup>2</sup>*The Ohio State University*

# Structure-Property Linkage: Plastic Anisotropy in Metals

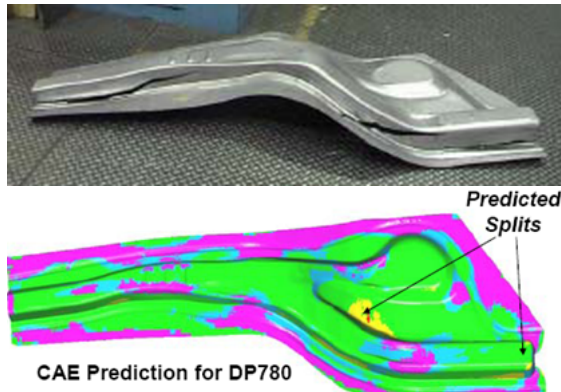


Polycrystalline microstructure

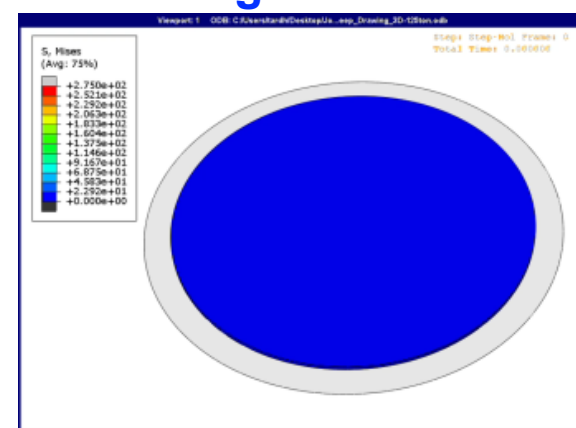


Change in grain morphology and **crystallographic texture**

## Accurate strength/formability predictions in metal forming

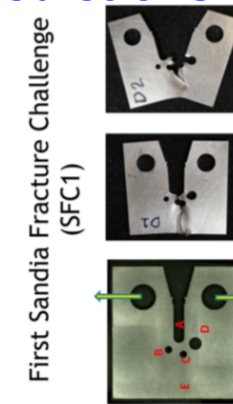


CAE Prediction for DP780

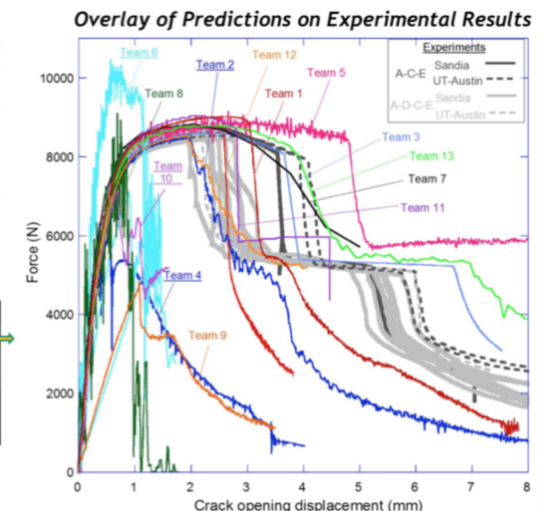


Deep drawing/ Forming simulations

## Accurate failure and fracture predictions

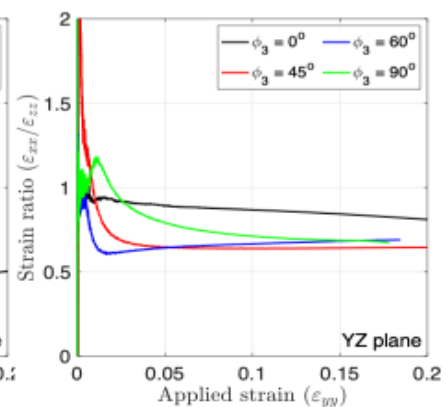
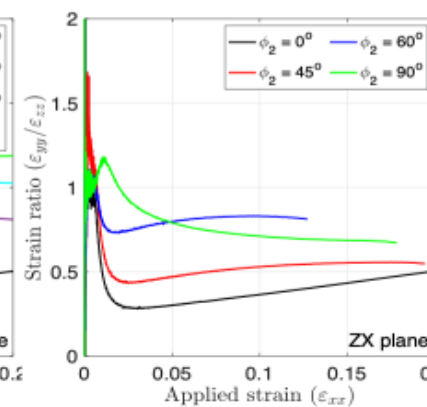
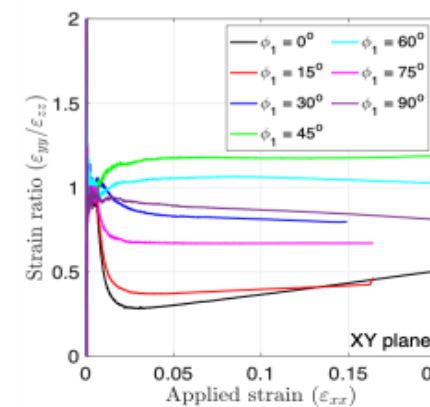
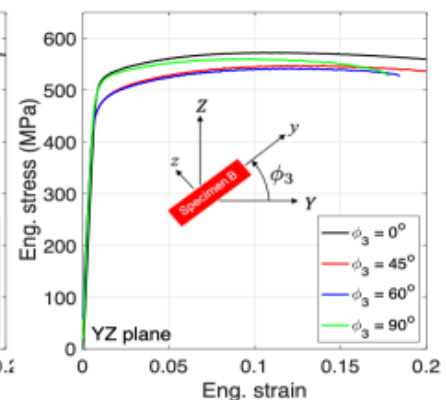
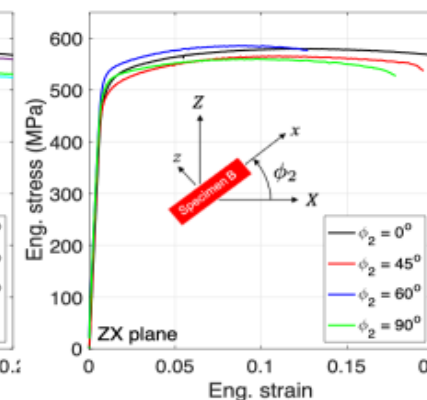
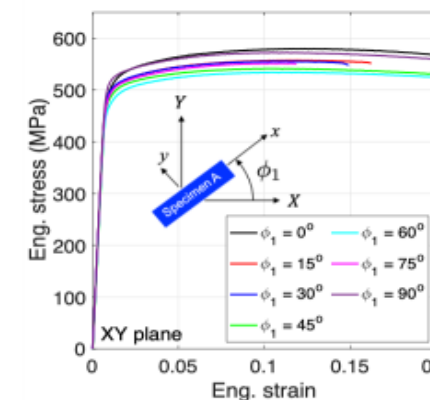
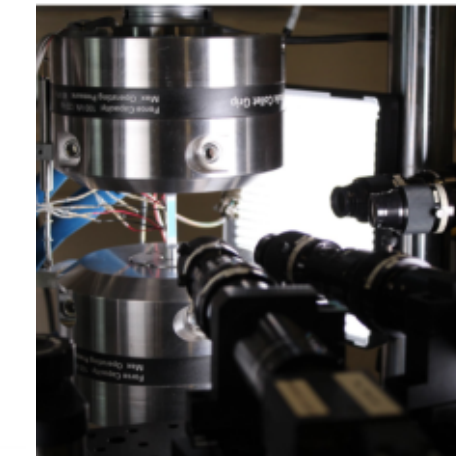
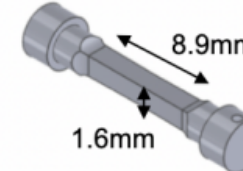
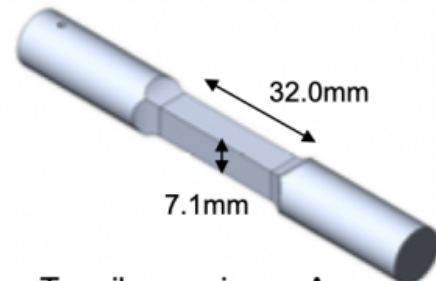
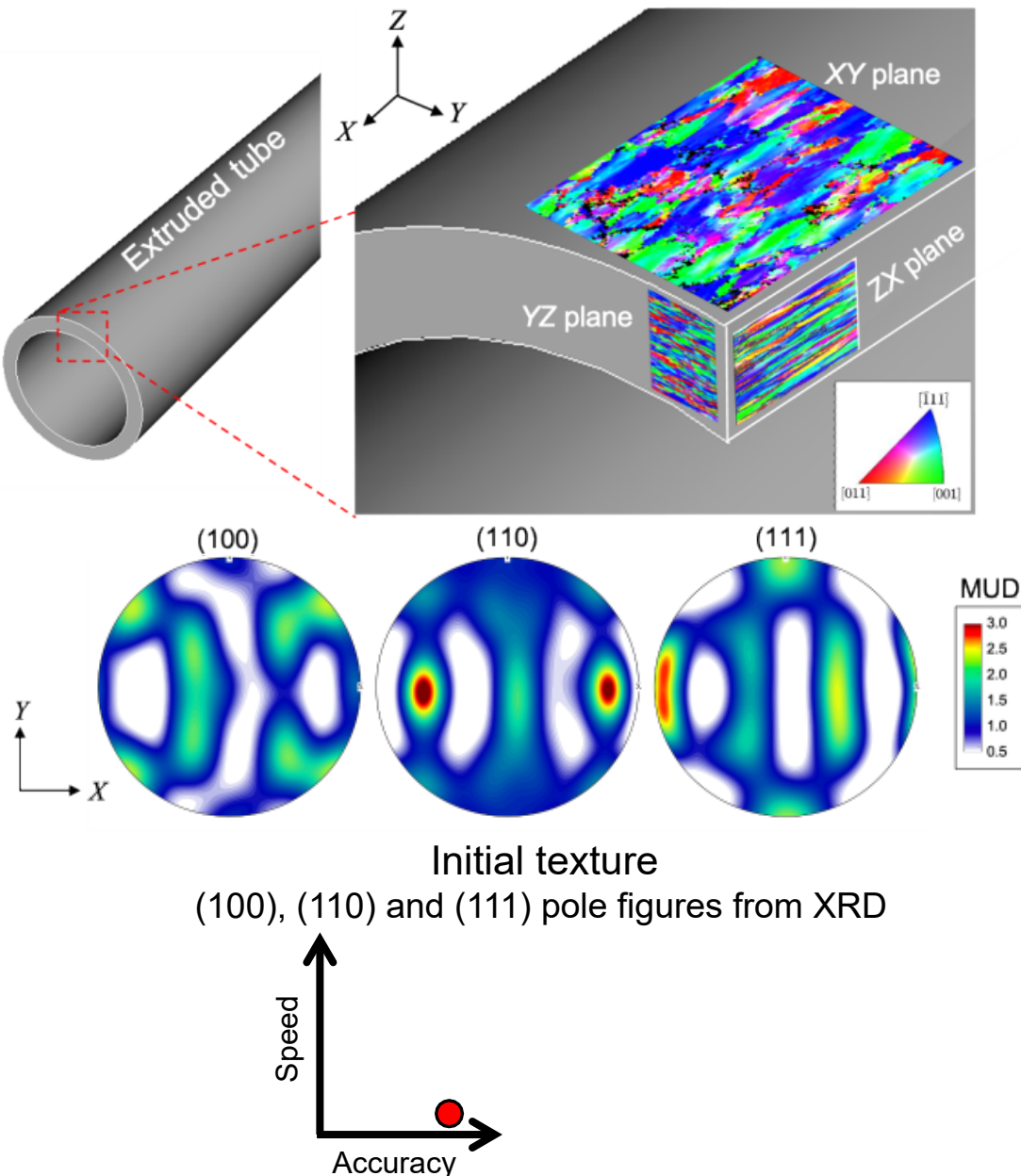


First Sandia Fracture Challenge (SFC1)



Sandia Fracture Challenge (Kramer et al., 2018)

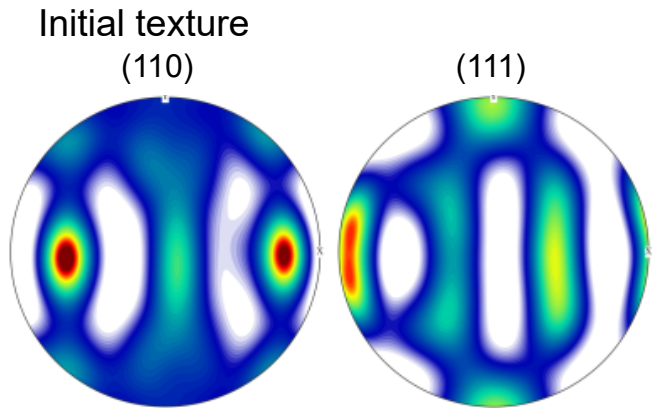
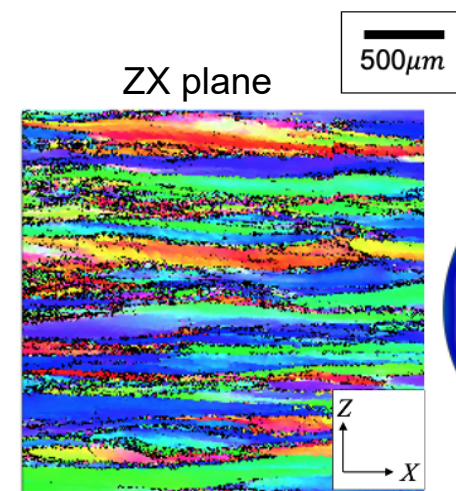
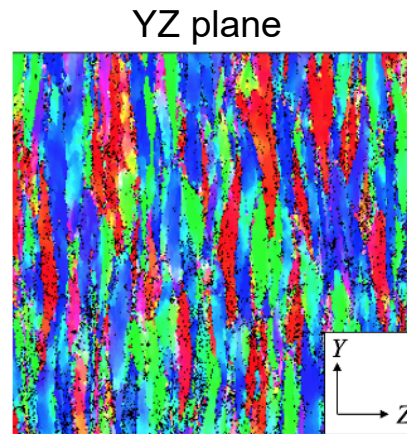
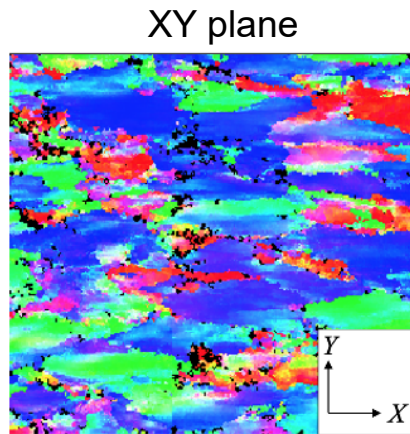
## Structure-Property Linkage: Experimental Characterization of Anisotropy – Al7079



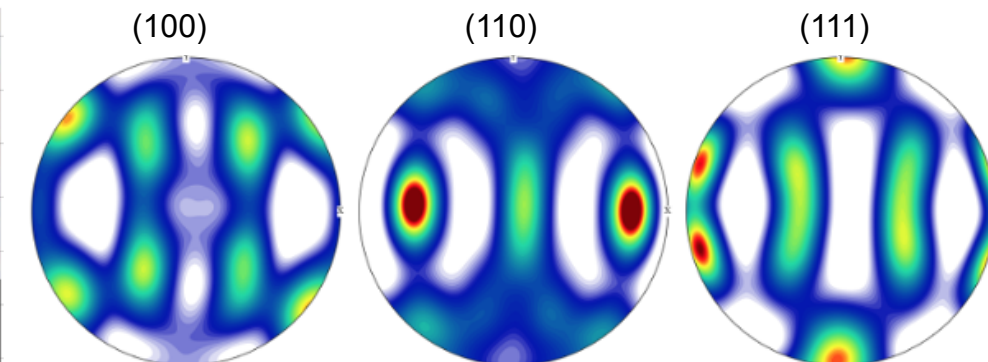
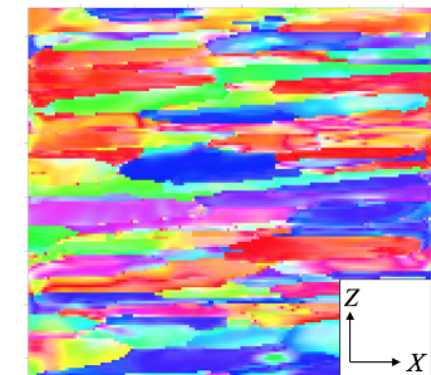
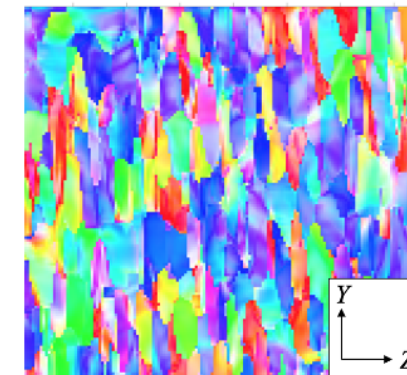
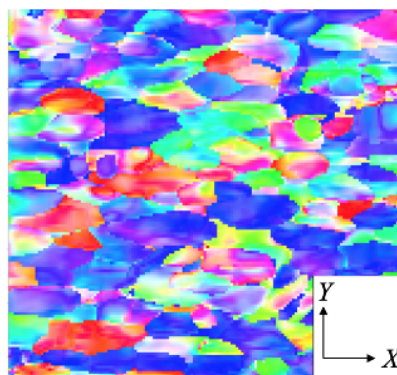
# Structure-Property Linkage: A computational Approach to Anisotropy Characterization



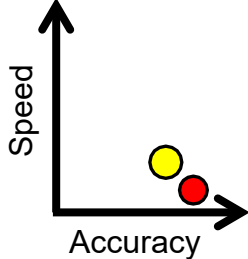
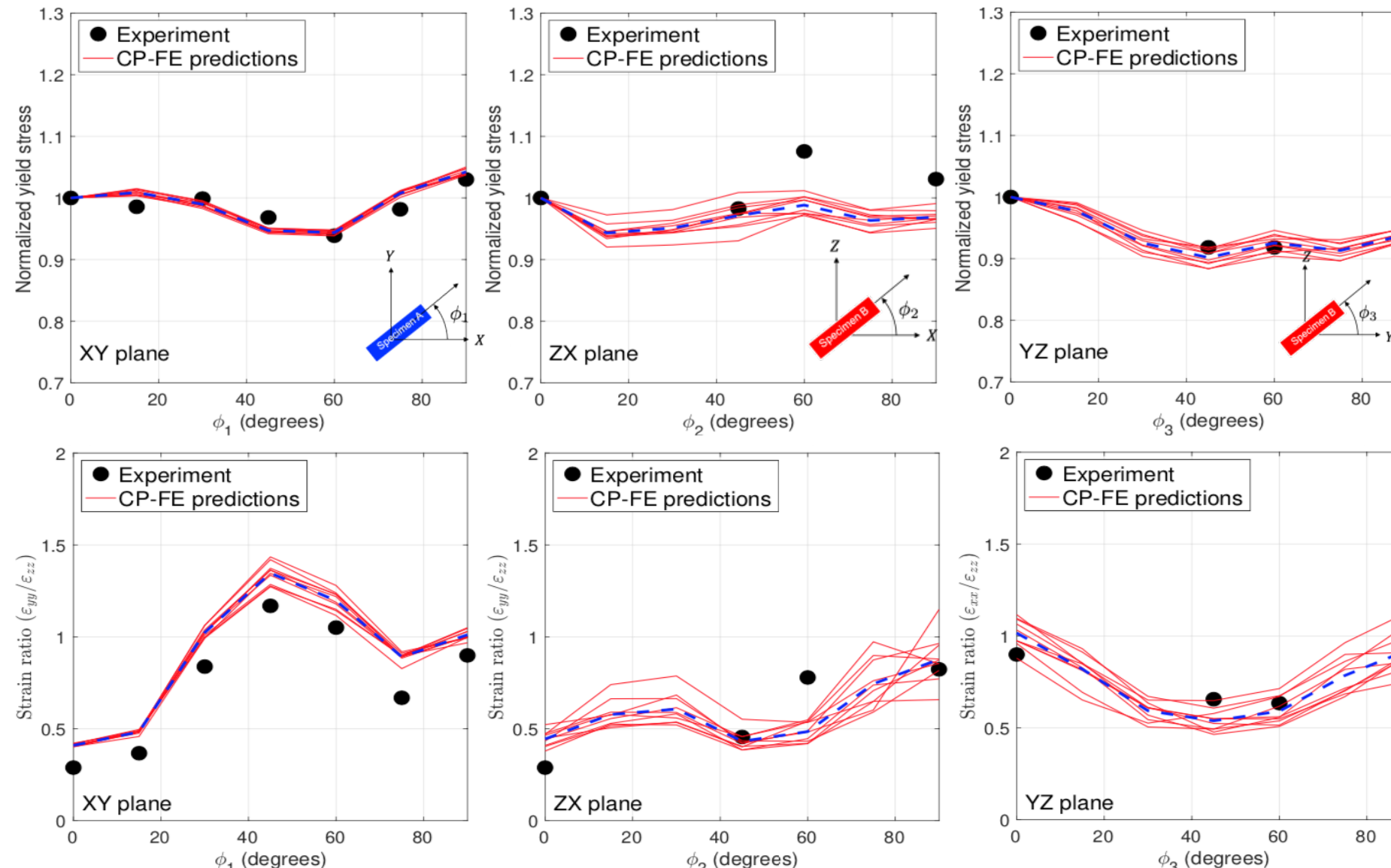
EBSD



Simulated Texture



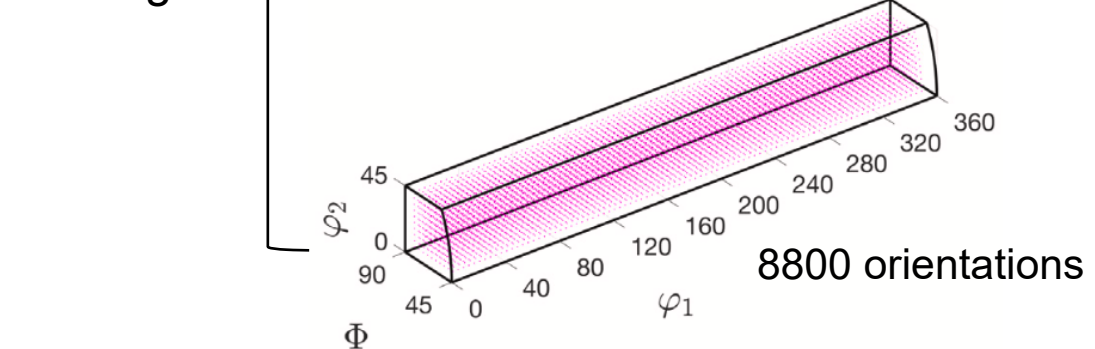
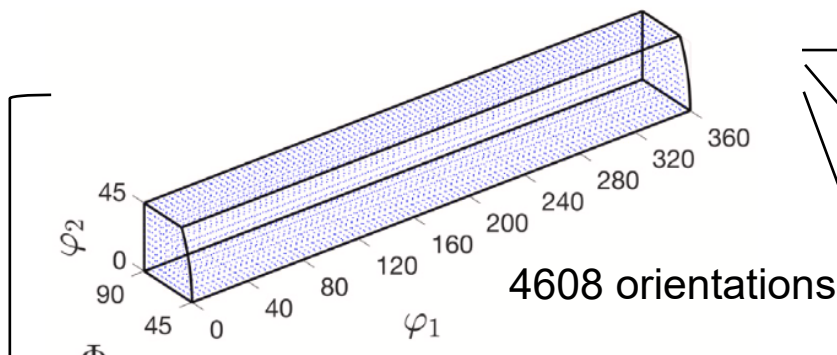
# Structure-Property Linkage: Computational predictions of Yield stress/ lateral strain ratio



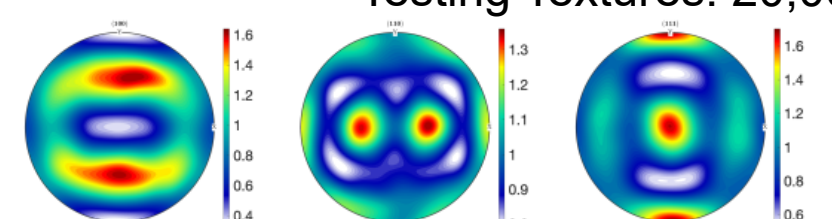
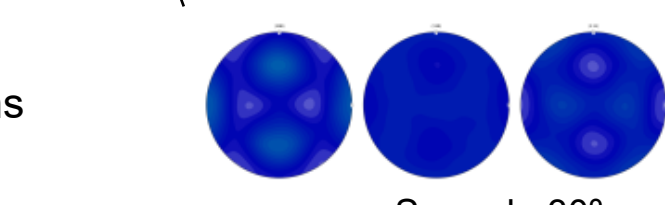
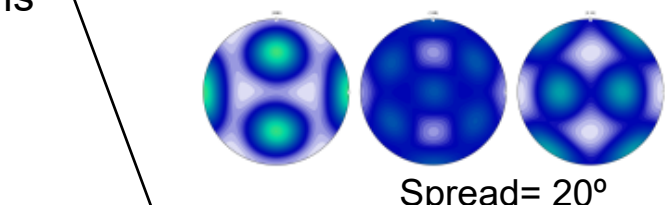
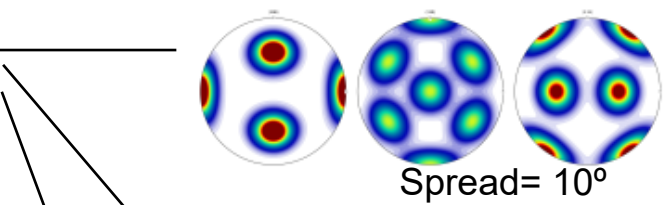
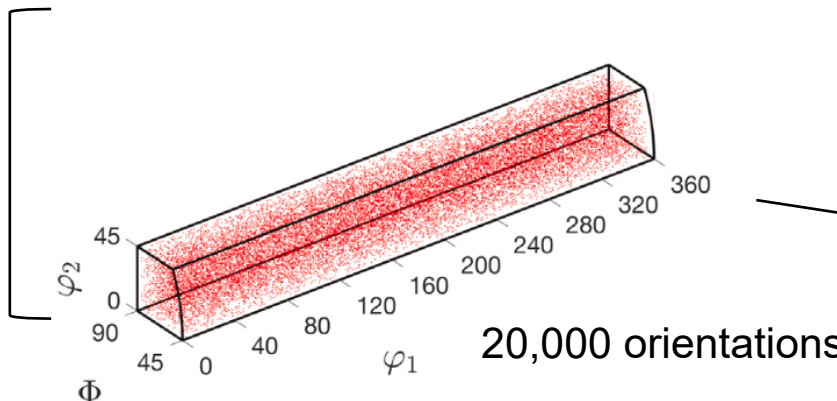
# Structure-Property Linkage: Using computational approaches to generate diverse training sets



54,880  
training set



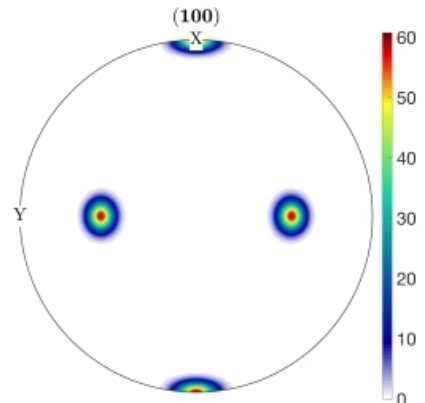
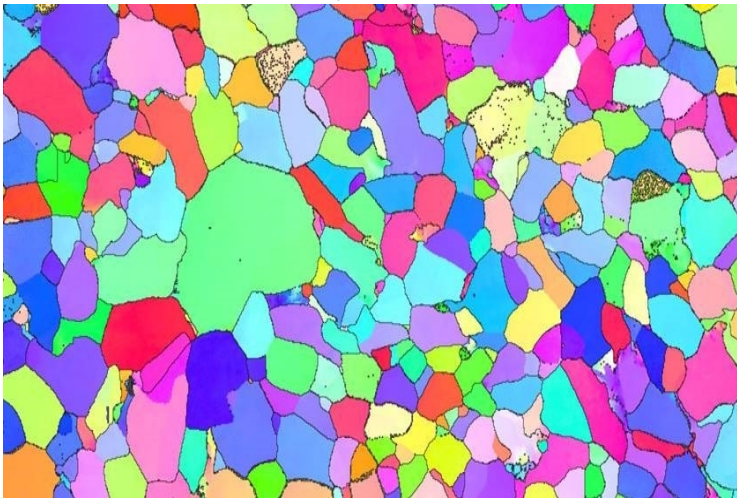
20,000  
testing set



# Surrogate Model: *Obtaining Fingerprint Descriptor*



Colors denote the crystal lattice orientation



$f_s(g)$  is the probability distribution of the orientation of the crystal lattice.

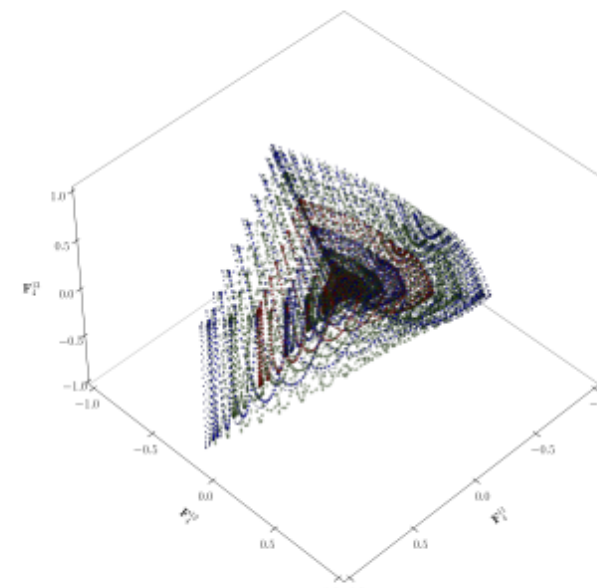
## Fourier Series Representation:

$$T_l^{\mu n}(g) = T_l^{\mu n}(\varphi_1, \Phi, \varphi_2) = e^{im\varphi_1} P_l^{\mu n}(\Phi) e^{in\varphi_2}$$

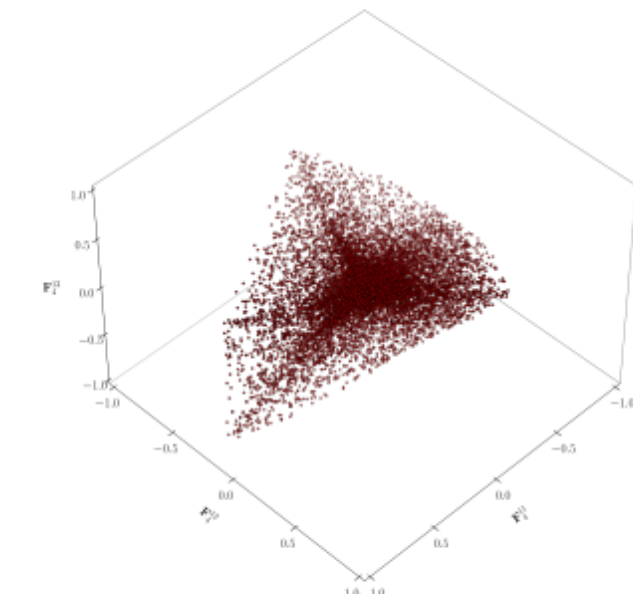
$$f_s(g) = \sum_{\mu, n, l} F_{ls}^{\mu n} T_l^{\mu n}(g),$$

- Orthogonal Basis functions basis functions
- Customized to account for symmetry.

$$F_{ls}^{\mu n} = (2l + 1) \int_{FZ} f_s(g) T_l^{\mu n*}(g) dg$$

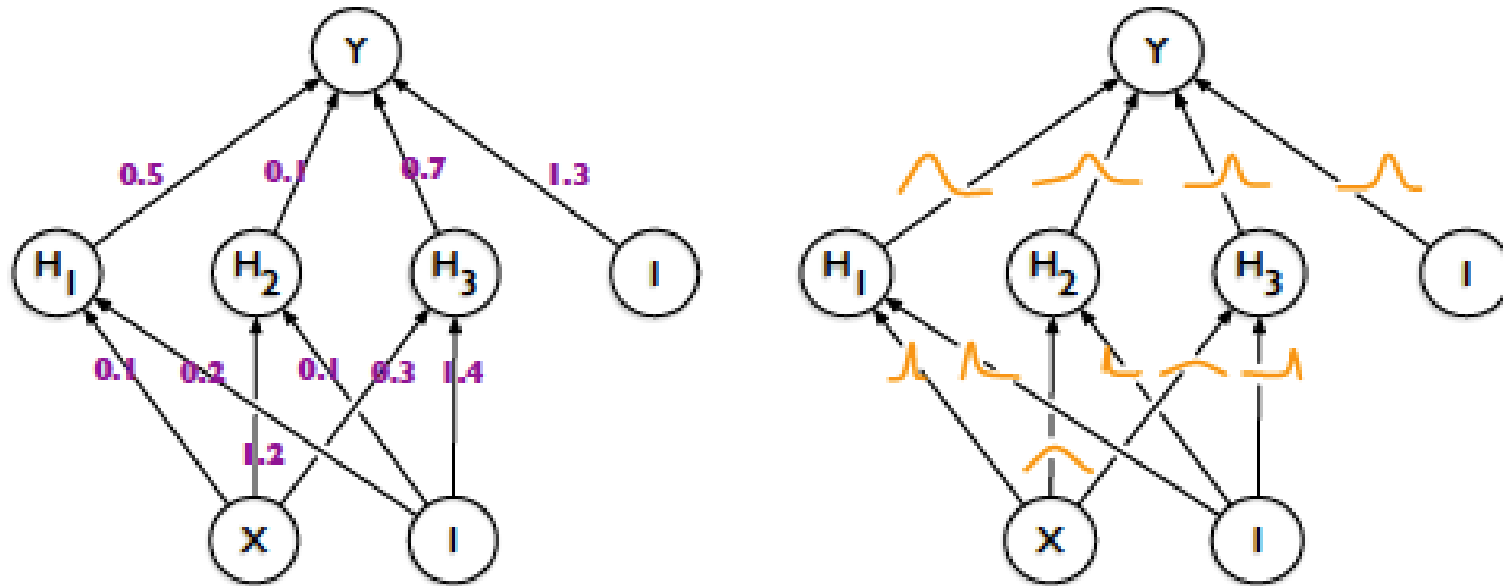


GSH representation of Training Textures



GSH representation of Testing Textures

## Surrogate Model: Neural Network Linkage

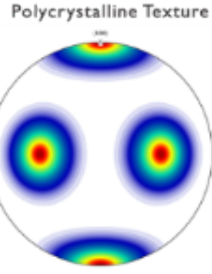


- Architecture of 2 hidden layers with 81 nodes on each layer and sigmoid activation function to predict the output with a GSH truncation level of  $l=12$ .
- Monte Carlo Sampling of 50 samples to obtain the distribution of weights, which in turn yielded a distribution of output values.
- Architecture trained to 5000 epochs.

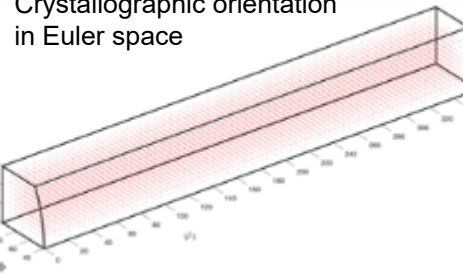
# 9 | Deep Learning Anisotropy Predictions: Hill's model



## Crystallographic textures



Crystallographic orientation  
in Euler space

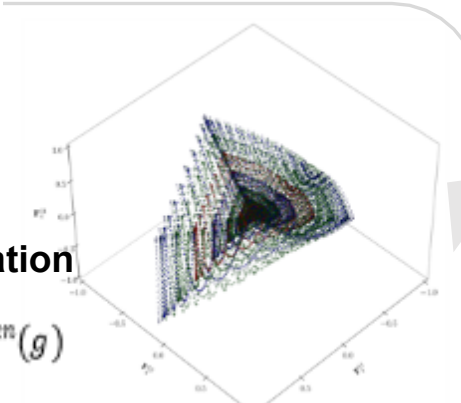


54,880 textures represented by  
generalized spherical harmonics (GSH)

## Texture quantification

$$f(g) = \sum_{\mu, n, l} F_l^{\mu n} T_l^{\mu n}(g)$$

$$T_l^{\mu n}(g) = T_l^{\mu n}(\varphi_1, \phi, \varphi_2) = e^{im\varphi_1} P_l^{\mu n}(\phi) e^{im\varphi_2}$$



## Variational Bayesian Inference Neural Network Model

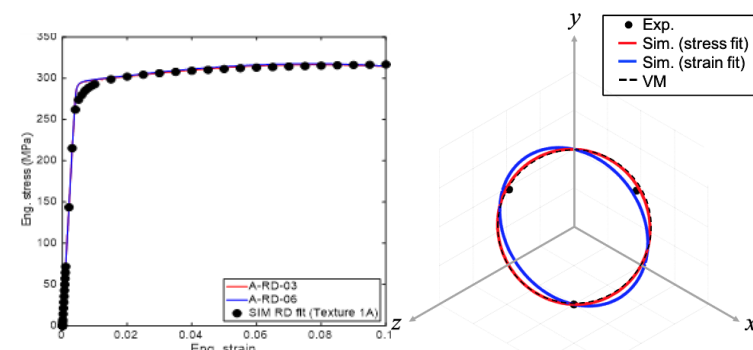


54,880 training data  
20,000 validation  
data

## Anisotropy Constants

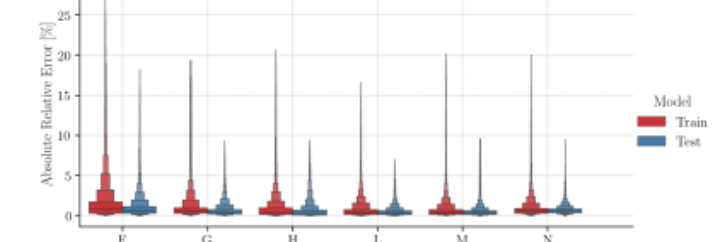
### Crystal plasticity simulations

54,880 crystal plasticity simulations  
performed to investigate anisotropic  
yield behavior and to fit Hill's anisotropy  
yield model



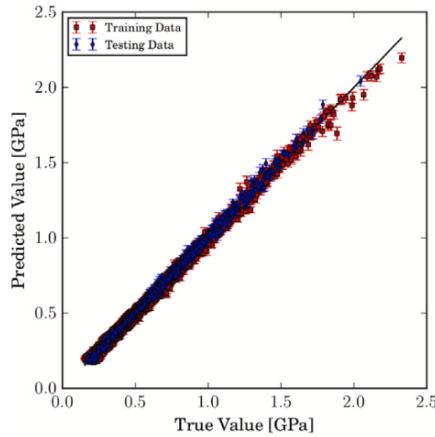
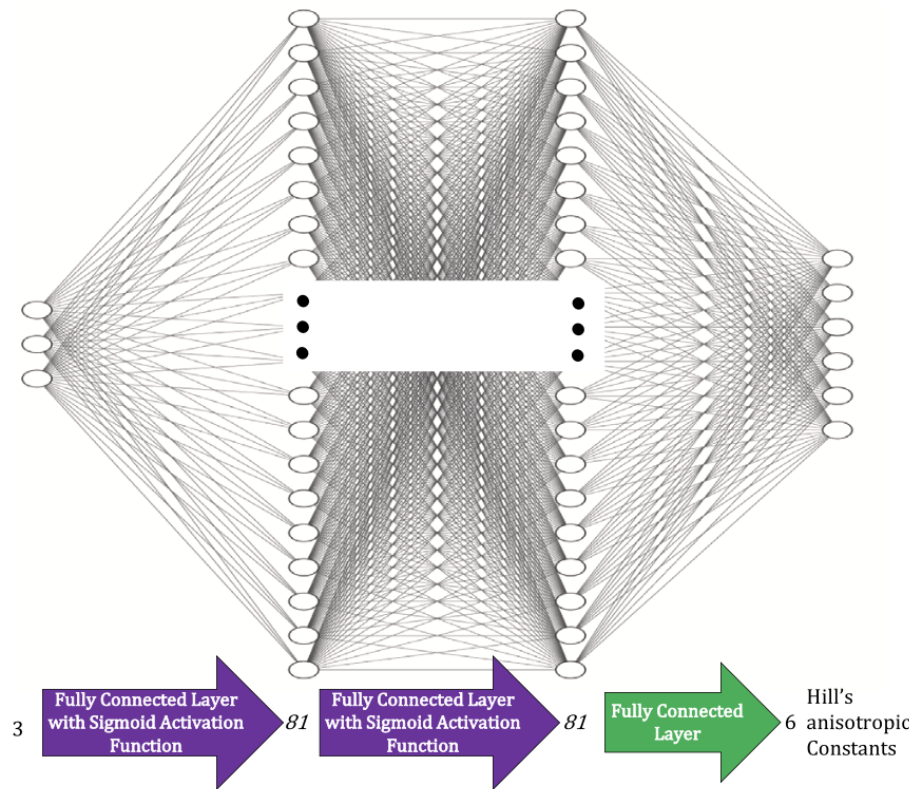
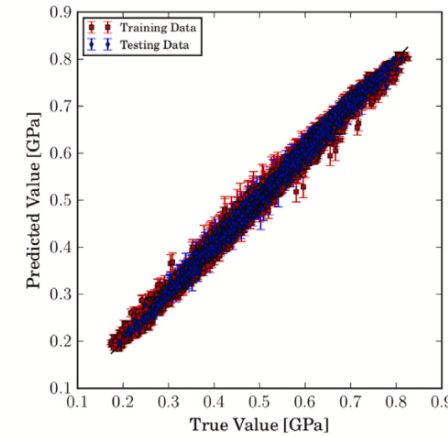
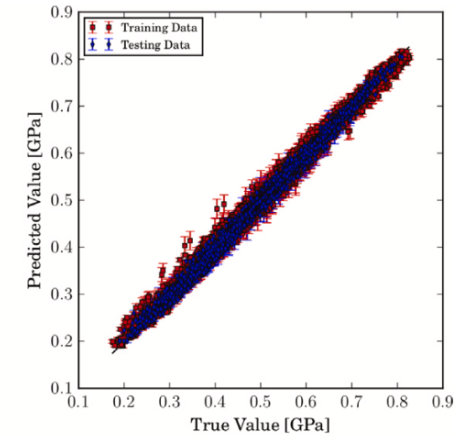
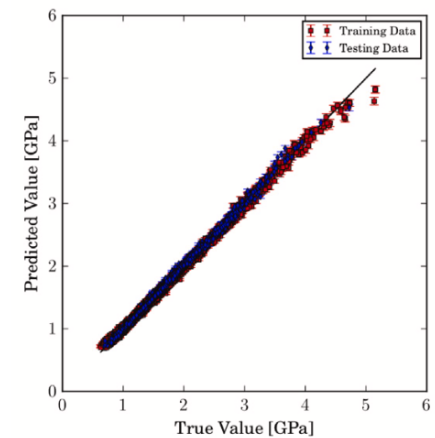
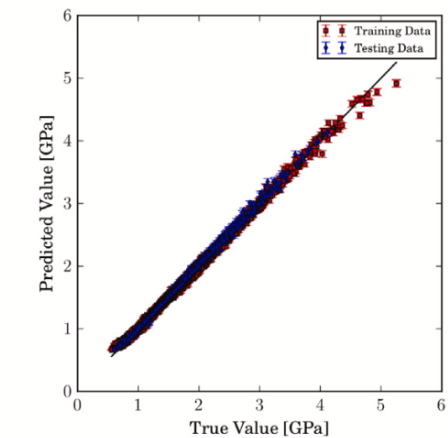
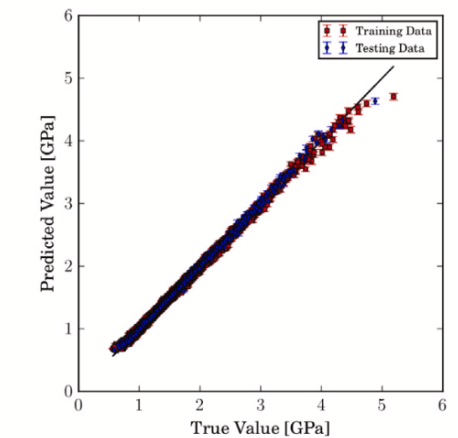
$$f = \textcolor{red}{F}(\sigma_{yy} - \sigma_{zz})^2 + \textcolor{red}{G}(\sigma_{zz} - \sigma_{xx})^2 + \textcolor{red}{H}(\sigma_{xx} - \sigma_{yy})^2 + 2(\textcolor{red}{L}\sigma_{yz}^2 + \textcolor{red}{M}\sigma_{zx}^2 + \textcolor{red}{N}\sigma_{xy}^2)$$

## Distribution of absolute relative error on the training and testing set



The mean error = 0.63%

# Deep Learning Model: Results

(a) *F*(b) *G*(c) *H*(d) *L*(e) *M*(f) *N*

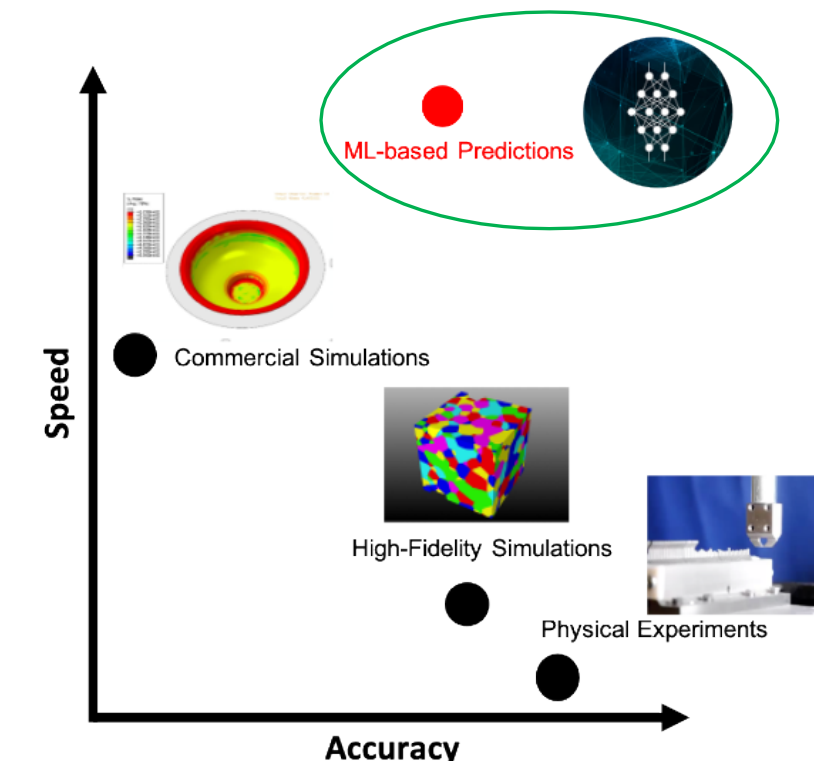
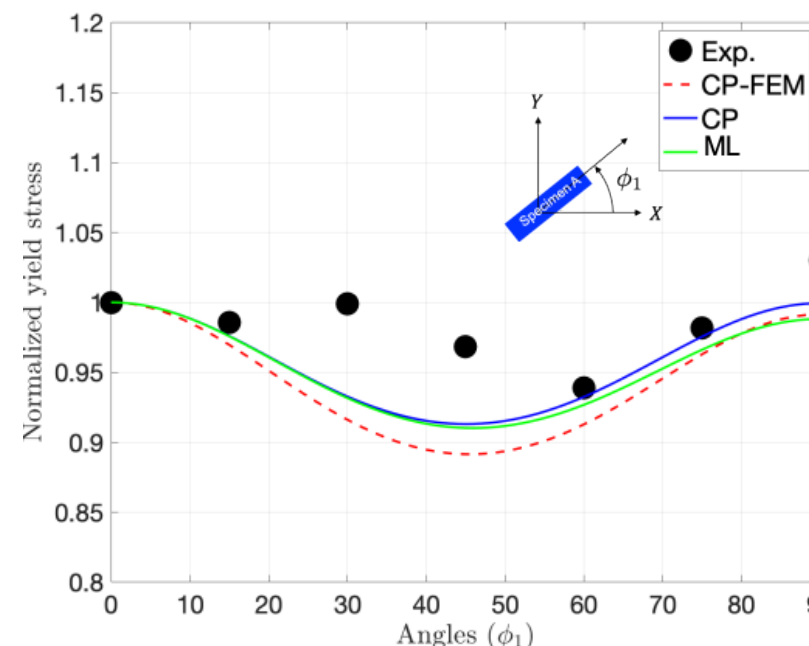
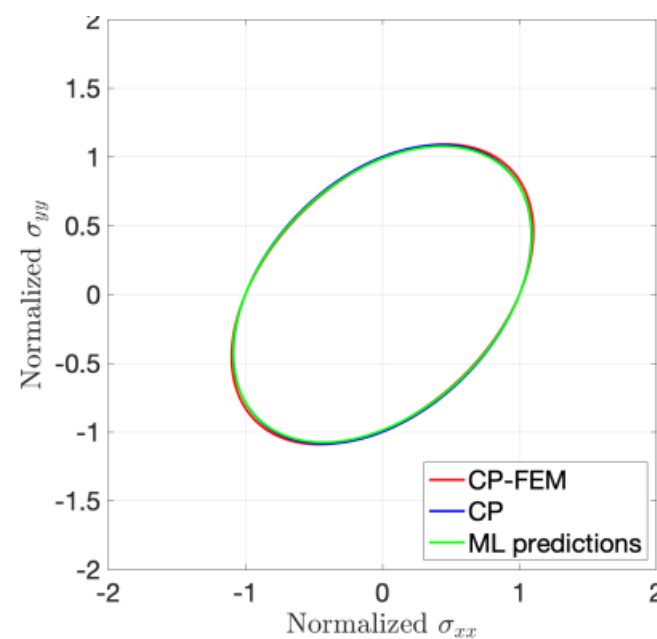
$$f = \textcolor{red}{F}(\sigma_{yy} - \sigma_{zz})^2 + \textcolor{red}{G}(\sigma_{zz} - \sigma_{xx})^2 + \textcolor{red}{H}(\sigma_{xx} - \sigma_{yy})^2 + 2(\textcolor{red}{L}\sigma_{yz}^2 + \textcolor{red}{M}\sigma_{zx}^2 + \textcolor{red}{N}\sigma_{xy}^2)$$

# Deep Learning Model: Comparisons with Experiments & CP simulations

11

Parameterizing Hill's quadratic anisotropic yield model  $\textcolor{red}{E}(\sigma_{yy} - \sigma_{zz})^2 + \textcolor{red}{G}(\sigma_{zz} - \sigma_{xx})^2 + \textcolor{red}{H}(\sigma_{xx} - \sigma_{yy})^2 + 2(\textcolor{red}{L}\sigma_{yz}^2 + \textcolor{red}{M}\sigma_{zx}^2 + \textcolor{red}{N}\sigma_{xy}^2)$

AI7079	<i>F</i>	<i>G</i>	<i>H</i>	<i>L</i>	<i>M</i>	<i>N</i>
Crystal plasticity-FE (10 avg.)	0.5961	0.5788	0.4212	1.6133	1.8279	1.9291
Crystal plasticity (no FE)	0.6078	0.6067	0.3933	1.8898	1.7352	1.7920
Neural Network predictions	<b>0.6225</b> <b><math>\pm 0.0018</math></b>	<b>0.5984</b> <b><math>\pm 0.0013</math></b>	<b>0.4016</b> <b><math>\pm 0.0013</math></b>	<b>1.9128</b> <b><math>\pm 0.0017</math></b>	<b>1.8355</b> <b><math>\pm 0.0018</math></b>	<b>1.8035</b> <b><math>\pm 0.0022</math></b>



Variational Bayesian Inference Neural Network (VBI-NN) model of Hill's anisotropy model saves computational cost by an order of 1000 compared to crystal plasticity finite element simulations.

# Deep Learning Model: Generalized Anisotropy



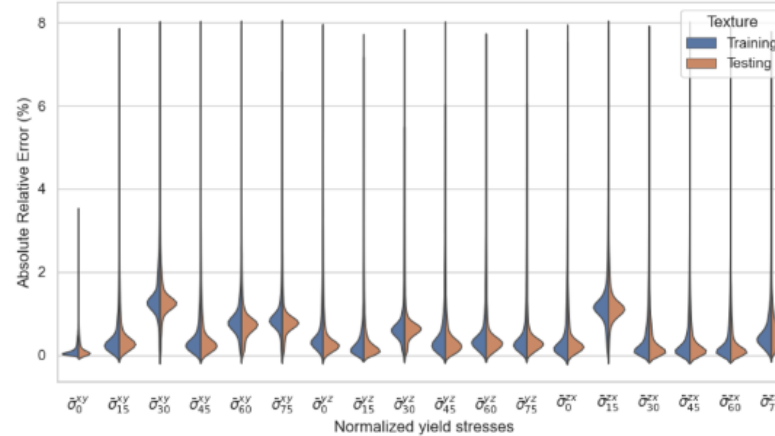
54,880 textures



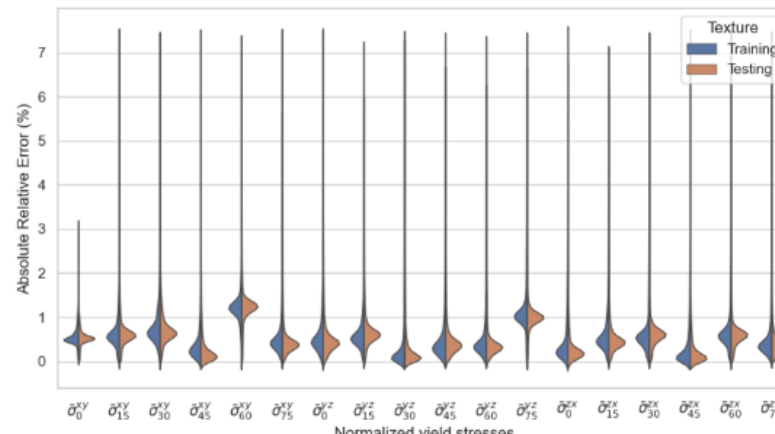
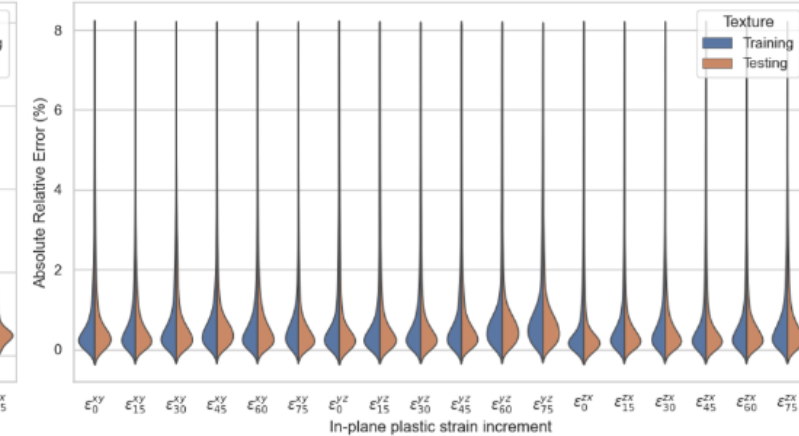
54 anisotropy parameters: 18 normalized yield stresses and 36 lateral strain increments

CP vs. ML error:

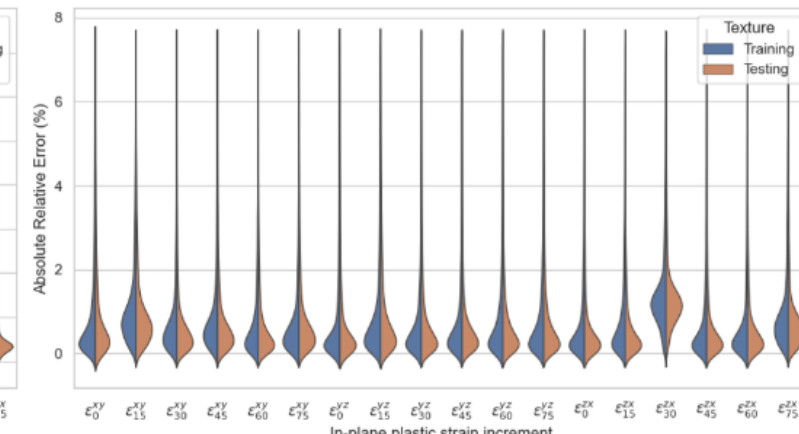
$$(Error_i)_j = \frac{|(y_i^{NN})_j - (y_i^{CP})_j|}{\sum_{j=1}^{N_{texture}} (y_i^{CP})_j} \times 100\%$$



(a) FCC



(b) BCC

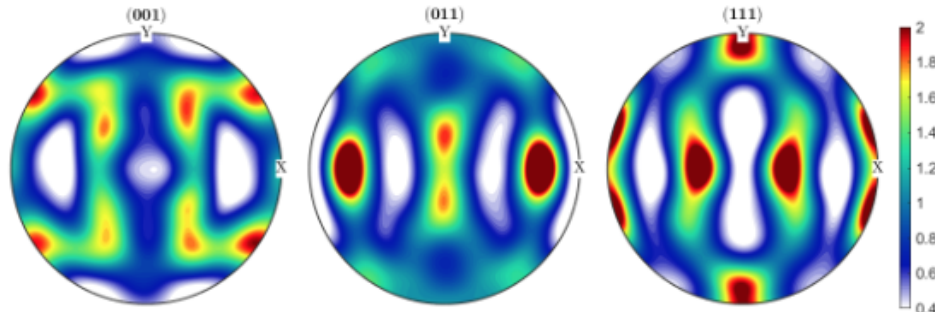


# Deep Learning Model: Application to Al5053 and Al7079

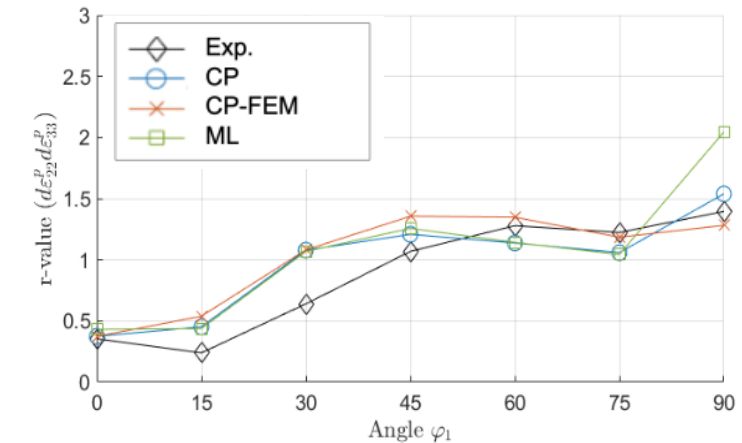
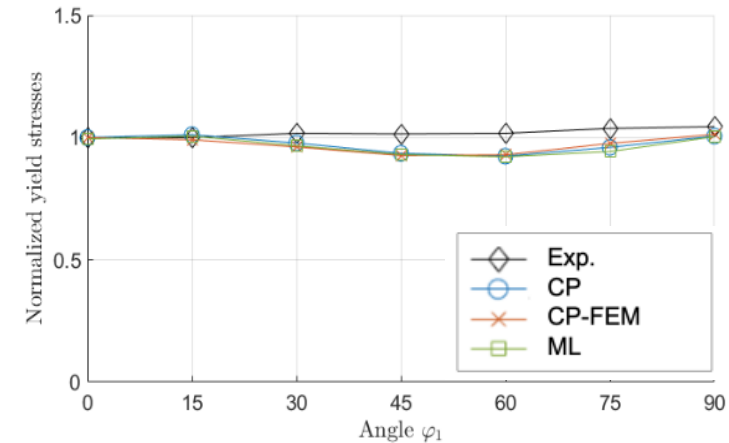
13



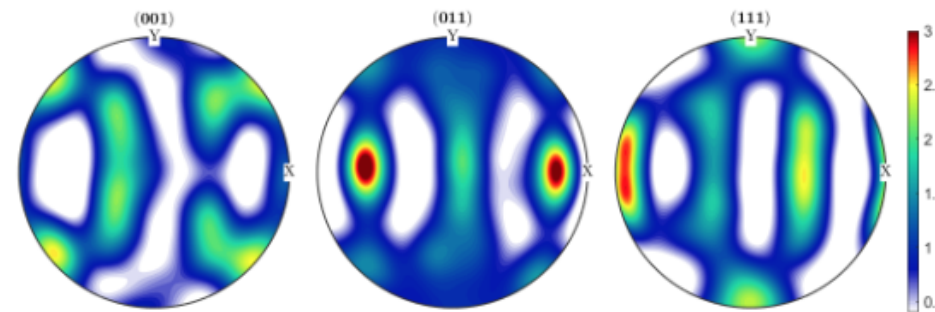
AA5053



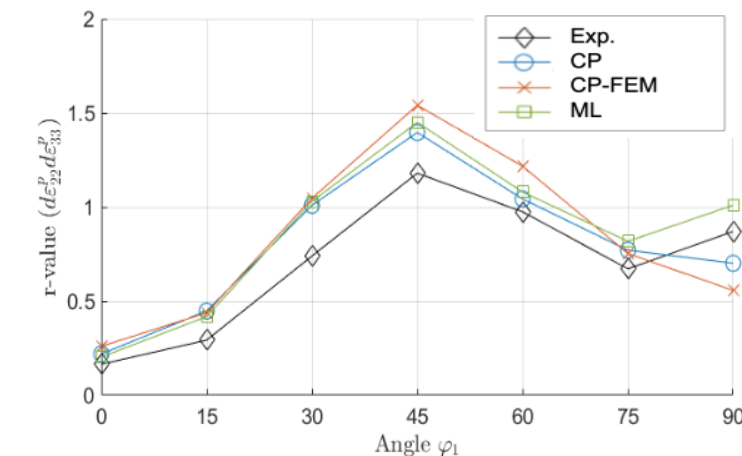
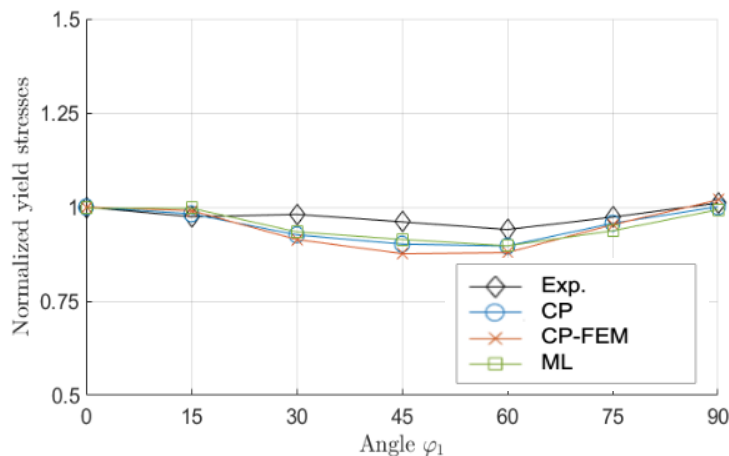
Initial texture



AA7079



Initial texture



# Deep Learning Model: Application to Cup Drawing FE Simulation

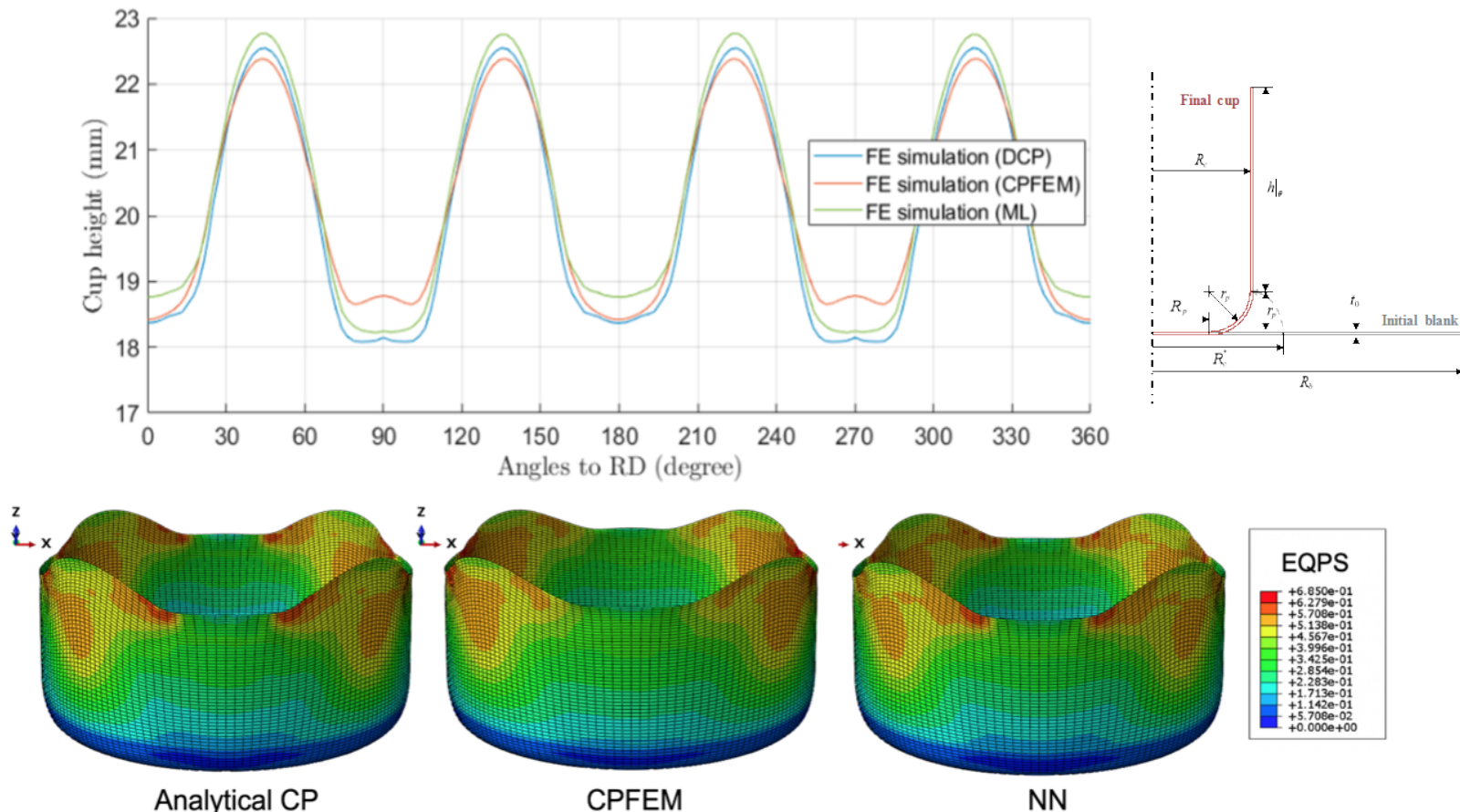
14



## Yld2004-18p parameters for AA5053 & AA7079

Material	AA5042			AA7079		
	ACP	CPFEM	DL	ACP	CPFEM	DL
$m$	8	8	8	8	8	8
$C'_{12}$	0.4619	0.2464	0.6263	1.0509	0.4302	0.7625
$C'_{13}$	0.8858	1.1305	0.9573	0.5351	1.1655	0.1462
$C'_{21}$	0.9848	1.0584	0.9338	1.1182	1.1990	0.7825
$C'_{23}$	1.2299	1.1221	1.2882	1.3488	1.2892	1.2530
$C'_{31}$	0.3762	0.3040	0.4930	1.0426	0.3258	1.1727
$C'_{32}$	1.3049	1.3922	1.1947	0.6300	1.2479	0.4980
$C'_{44}$	0.7878	0.4345	0.9902	1.2469	0.5231	1.0684
$C'_{55}$	1.6519	1.7722	1.1685	1.1925	1.7180	1.1753
$C'_{66}$	0.7217	0.8402	0.7628	1.4531	0.9517	0.8235
$C''_{12}$	0.7663	0.6731	0.8781	0.7356	0.5512	0.5213
$C''_{13}$	1.1852	1.2779	0.9823	1.2552	1.1326	1.0376
$C''_{21}$	0.8840	0.5907	0.9893	0.5836	0.8244	0.1518
$C''_{23}$	0.3346	0.1738	0.4572	1.2941	0.5072	-0.7896
$C''_{31}$	1.3246	1.1097	1.2353	0.7653	1.1498	0.4781
$C''_{32}$	0.6090	0.2081	0.7023	0.5736	0.4899	-0.7788
$C''_{44}$	1.2503	1.5792	1.0723	0.8948	1.4978	1.1589
$C''_{55}$	0.3369	0.0008	0.8386	0.8995	0.2875	1.0046
$C''_{66}$	1.3630	1.2791	1.3378	0.6968	1.2489	1.4670

## Earing profiles of Al5053



ABAQUS/Explicit  
4-node shell element  
Blank holding force = 8.9 kN

# Energy I-CORPS: *Developing Data-Driven Frameworks Collaboratively*



# Energy I-CORPS: Knowledge Sharing with Industry and Academia



**75 Interviews**  
125 Interviewees  
43 Institutions  
8 Countries



## Industry Lag Time

Up to 6 months and specialized equipment to test materials.



## Forced to Use Existing Data

Use anisotropy measurements from a database of previously performed characterizations.



## Capital intensive solution

Resultant simulations are not accurate. Consequently, need to perform forming trials.



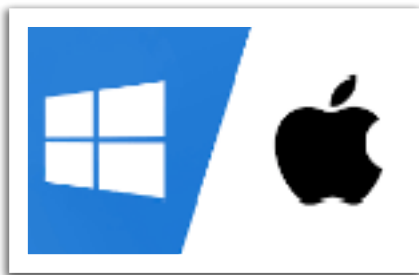
## Massive Carbon Footprint

Mechanical test requires wasting tons of materials, transporting materials, and disposing of wasted materials.

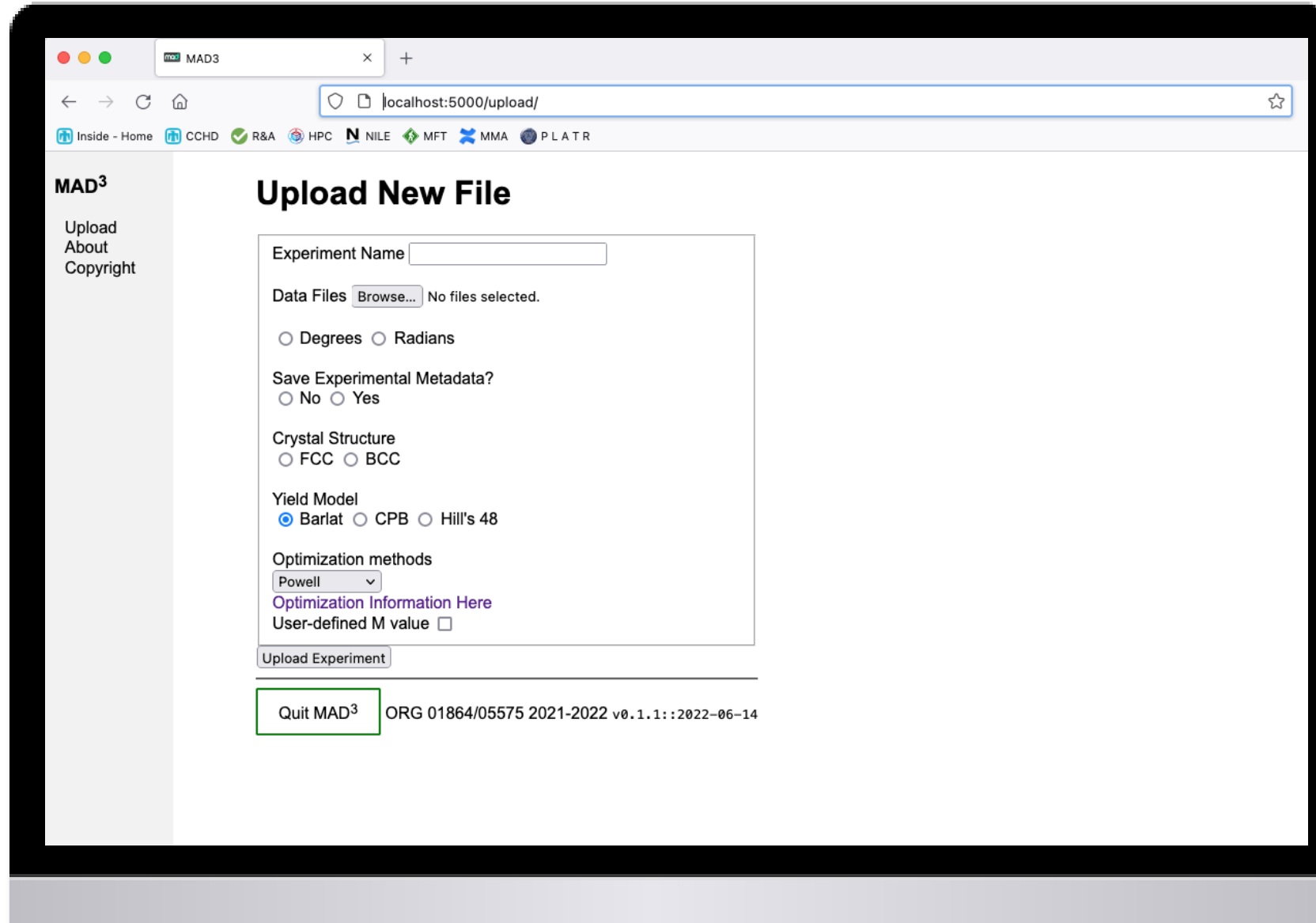


# MAD<sup>3</sup>: Packaging our research work into a easy-to-use GUI

17



Mac/Windows compatible

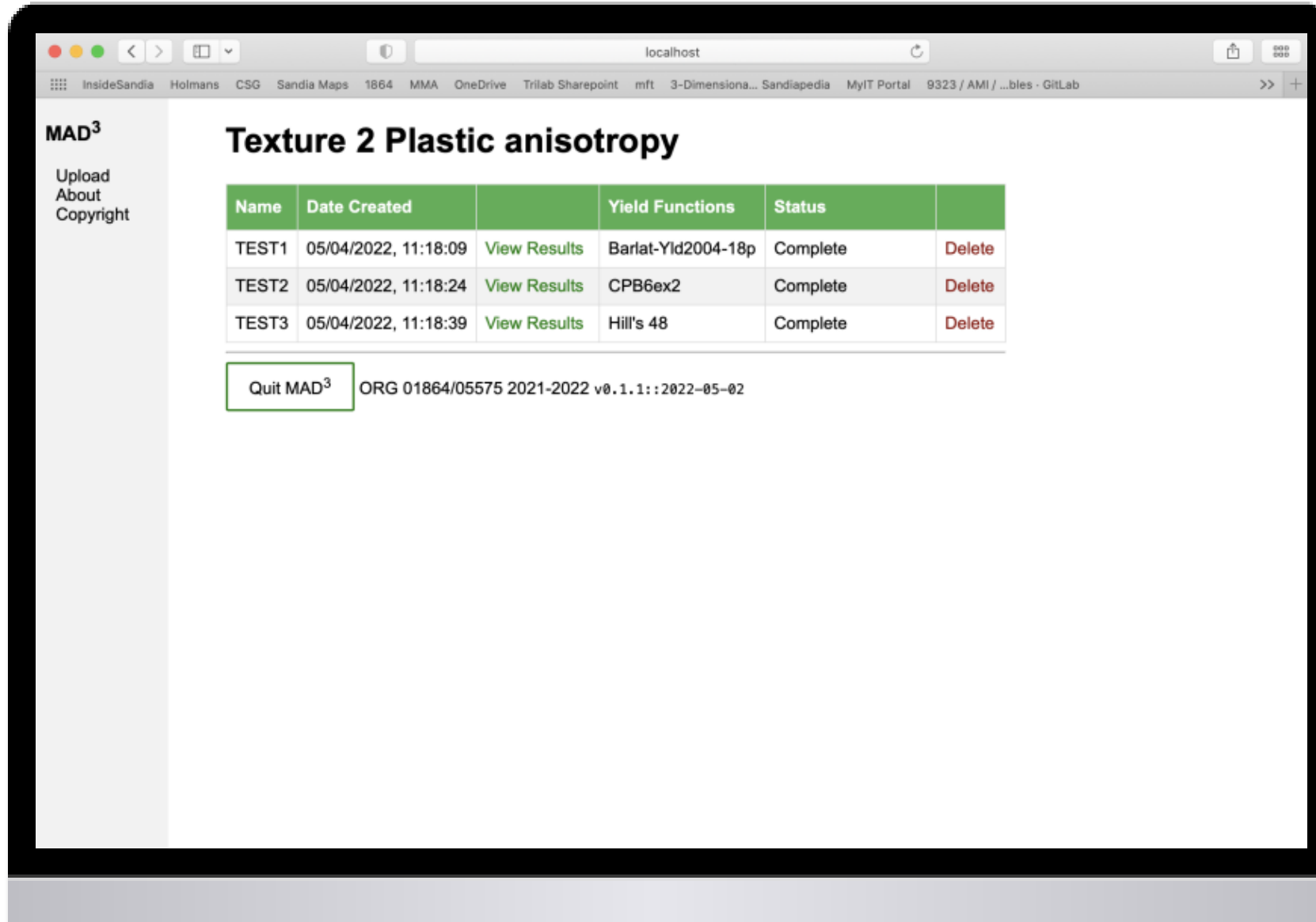
A screenshot of a web browser window titled "mad MAD3" showing the "Upload New File" interface. The browser address bar shows "localhost:5000/upload/". The interface includes a sidebar with "MAD3", "Upload", "About", and "Copyright" links. The main form contains fields for "Experiment Name" (with a placeholder "Experiment Name"), "Data Files" (with a "Browse..." button and a note "No files selected."), and "Angle Units" (radio buttons for "Degrees" and "Radians"). It also includes sections for "Save Experimental Metadata?" (radio buttons for "No" and "Yes"), "Crystal Structure" (radio buttons for "FCC" and "BCC"), "Yield Model" (radio buttons for "Barlat", "CPB", and "Hill's 48" with "Barlat" selected), "Optimization methods" (a dropdown menu showing "Powell" with a downward arrow), and a link "Optimization Information Here". There is also a checkbox for "User-defined M value". At the bottom of the form is a "Upload Experiment" button. At the very bottom of the browser window is a footer bar with a "Quit MAD3" button and the text "ORG 01864/05575 2021-2022 v0.1.1::2022-06-14".

# MAD<sup>3</sup>: Packaging our research work into a easy-to-use GUI

18



Mac/Windows compatible

A screenshot of a web browser window titled "localhost" showing the MAD<sup>3</sup> software interface. The left sidebar has links for "MAD<sup>3</sup>", "Upload", "About", and "Copyright". The main content area is titled "Texture 2 Plastic anisotropy" and displays a table of test results. The table has columns for Name, Date Created, Yield Functions, and Status. Each row contains a "View Results" link. The data in the table is as follows:

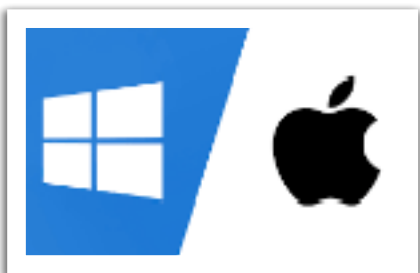
Name	Date Created	Yield Functions	Status	
TEST1	05/04/2022, 11:18:09	View Results Barlat-Yld2004-18p	Complete	Delete
TEST2	05/04/2022, 11:18:24	View Results CPB6ex2	Complete	Delete
TEST3	05/04/2022, 11:18:39	View Results Hill's 48	Complete	Delete

At the bottom left is a "Quit MAD<sup>3</sup>" button, and at the bottom center is the text "ORG 01864/05575 2021-2022 v0.1.1::2022-05-02".

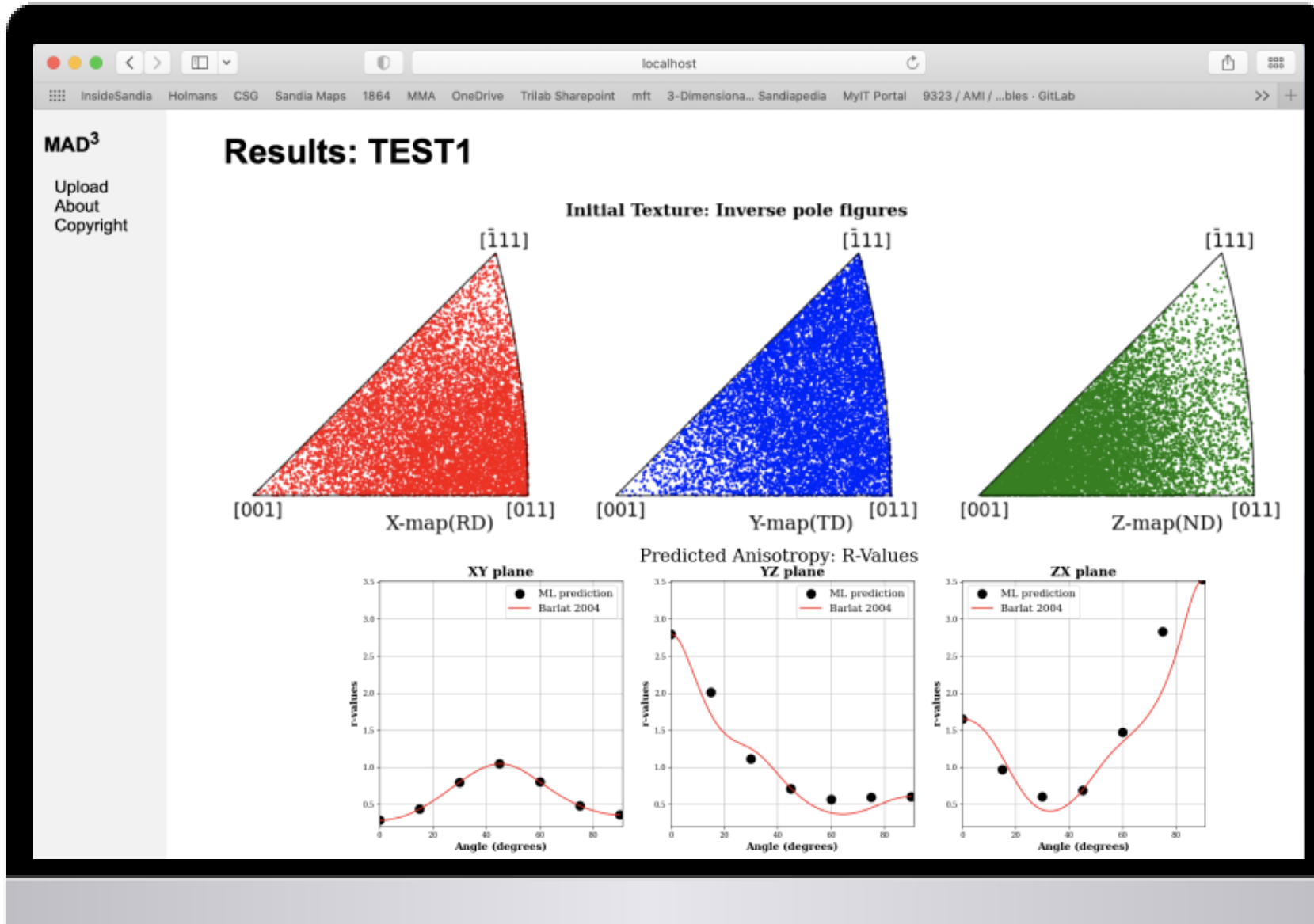


# MAD<sup>3</sup>: Packaging our research work into a easy-to-use GUI

19



Mac/Windows compatible



Licensing: IP@SANDIA.GOV

DOE Software Copyright Assertion



# MAD<sup>3</sup>: Packaging our research work into a easy-to-use GUI

20



Mac/Windows compatible

Normalized Yield Stress

$\sigma_{00}^N$	$\sigma_{11}^N$	$\sigma_{33}^N$	$\sigma_{44}^N$	$\sigma_{60}^N$	$\sigma_{70}^N$	$\sigma_{50}^N$	$\sigma_{13}^N$	$\sigma_{31}^N$	$\sigma_{45}^N$	$\sigma_{60}^N$	$\sigma_{15}^N$	$\sigma_{20}^N$	$\sigma_{30}^N$	$\sigma_{40}^N$	$\sigma_{50}^N$	$\sigma_{60}^N$	$\sigma_{70}^N$
1.0	0.9942	0.9738	0.9745	0.9853	1.0152	1.038	1.0405	1.0592	1.0578	1.0202	0.9942	0.9928	0.9891	1.0151	1.0817	1.081	1.0304

Lateral Strain 1 (in-plane)

$\epsilon_{00}^H$	$\epsilon_{11}^H$	$\epsilon_{33}^H$	$\epsilon_{44}^H$	$\epsilon_{60}^H$	$\epsilon_{70}^H$	$\epsilon_{50}^H$	$\epsilon_{13}^H$	$\epsilon_{31}^H$	$\epsilon_{45}^H$	$\epsilon_{60}^H$	$\epsilon_{15}^H$	$\epsilon_{20}^H$	$\epsilon_{30}^H$	$\epsilon_{40}^H$	$\epsilon_{50}^H$	$\epsilon_{60}^H$	$\epsilon_{70}^H$
-0.2198	-0.3066	-0.4509	-0.5221	-0.4532	-0.3209	-0.7112	-0.6348	-0.5006	-0.3975	-0.3538	-0.3767	-0.6394	-0.5031	-0.3654	-0.3792	-0.552	-0.400

Lateral Strain 2 (normal to plane)

$\epsilon_{00}^V$	$\epsilon_{11}^V$	$\epsilon_{33}^V$	$\epsilon_{44}^V$	$\epsilon_{60}^V$	$\epsilon_{70}^V$	$\epsilon_{50}^V$	$\epsilon_{13}^V$	$\epsilon_{31}^V$	$\epsilon_{45}^V$	$\epsilon_{60}^V$	$\epsilon_{15}^V$	$\epsilon_{20}^V$	$\epsilon_{30}^V$	$\epsilon_{40}^V$	$\epsilon_{50}^V$	$\epsilon_{60}^V$	$\epsilon_{70}^V$
-0.7768	-0.7021	-0.5684	-0.4985	-0.5649	-0.6668	-0.2544	-0.3155	-0.4485	-0.5569	-0.6247	-0.6294	-0.3868	-0.5181	-0.603	-0.5507	-0.3749	-0.400

Optimized parameters for Barlat Yld2004-18p (Barlat et al., 2005)

$c'_{12}$	$c'_{13}$	$c'_{21}$	$c'_{23}$	$c'_{31}$	$c'_{32}$	$c'_{44}$	$c'_{55}$	$c'_{66}$	$c''_{12}$	$c''_{13}$	$c''_{21}$	$c''_{23}$	$c''_{31}$	$c''_{32}$	$c''_{44}$	$c''_{55}$	$c''_{66}$
0.2358	0.8113	0.7176	0.9674	0.9987	0.9872	0.9212	1.1197	0.8716	1.1107	1.2219	1.0687	0.1918	0.5613	1.1125	0.7516	0.5393	1.0855

Refresh Plots      Download Plots

Quit MAD<sup>3</sup>      ORG 01864/05575 2021-2022 v0.1.1::2022-05-02



# Summary

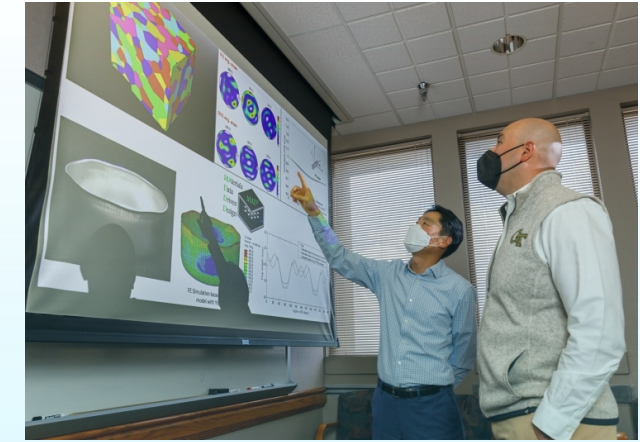


- CP-FEM simulations provide reasonable yield stresses and lateral strain ratio predictions.
- Deep Learning model was trained from CP data and showed good agreement in anisotropy predictions.
- Developed a GUI-based app that instantly predicts plastic anisotropy from initial texture.
- ML-based model provides a convenient & direct link from *material's **microstructure** to macro-scale **anisotropy*** of metals.

# THANK YOU!



[https://newsreleases.sandia.gov/quality\\_testing/](https://newsreleases.sandia.gov/quality_testing/)



**David Montes de Oca Zapiain:** [dmonte@sandia.gov](mailto:dmonte@sandia.gov)  
**Hojun Lim:** [hnlim@sandia.gov](mailto:hnlim@sandia.gov)



### 1. Hill 1948 function (6 coefficients) [1]

$$f = \bar{\sigma}^2 = (G + H)\sigma_{xx}^2 + (H + F)\sigma_{yy}^2 + (F + G)\sigma_{zz}^2 - 2(F\sigma_{yy}\sigma_{zz} + G\sigma_{zz}\sigma_{xx} + H\sigma_{xx}\sigma_{yy}) + 2(L\sigma_{yz}^2 + M\sigma_{zx}^2 + N\sigma_{xy}^2)$$

### 2. Yld2004-18p function (18+1 coefficients) [2]

$$f = 4\bar{\sigma}^a = |\tilde{S}'_1 - \tilde{S}''_1|^a + |\tilde{S}'_1 - \tilde{S}''_2|^a + |\tilde{S}'_1 - \tilde{S}''_3|^a + |\tilde{S}'_2 - \tilde{S}''_1|^a + |\tilde{S}'_2 - \tilde{S}''_2|^a + |\tilde{S}'_2 - \tilde{S}''_3|^a + |\tilde{S}'_3 - \tilde{S}''_1|^a + |\tilde{S}'_3 - \tilde{S}''_2|^a + |\tilde{S}'_3 - \tilde{S}''_3|^a$$

$\tilde{S}'_i$  and  $\tilde{S}''_i$  ( $i=1, 2$ , and  $3$ ) are principal components of the linearly transformed deviatoric stresses,  $\tilde{s}'$  and  $\tilde{s}''$ .

$$\tilde{s}' = \begin{bmatrix} s'_{xx} \\ s'_{yy} \\ s'_{zz} \\ s'_{xy} \\ s'_{yz} \\ s'_{zx} \end{bmatrix} = \mathbf{C}' \mathbf{s} = \begin{bmatrix} 0 & -c'_{12} & -c'_{13} & 0 & 0 & 0 \\ -c'_{21} & 0 & -c'_{23} & 0 & 0 & 0 \\ -c'_{31} & -c'_{32} & 0 & 0 & 0 & 0 \\ 0 & 0 & 0 & c'_{44} & 0 & 0 \\ 0 & 0 & 0 & 0 & c'_{55} & 0 \\ 0 & 0 & 0 & 0 & 0 & c'_{66} \end{bmatrix} \begin{bmatrix} s_{xx} \\ s_{yy} \\ s_{zz} \\ s_{yz} \\ s_{zx} \\ s_{xy} \end{bmatrix}$$

### 3. CPB06ex2 (18+1 coefficients) [3]

$$f = \bar{\sigma}^m = \frac{3^m}{2^{m+1}(1-k)^m + 4(1+k)^m} \left[ (\tilde{S}'_1 - k|\tilde{S}'_1|)^m + (\tilde{S}'_2 - k|\tilde{S}'_2|)^m + (\tilde{S}'_3 - k|\tilde{S}'_3|)^m + (\tilde{S}''_1 - k|\tilde{S}''_1|)^m + (\tilde{S}''_2 - k|\tilde{S}''_2|)^m + (\tilde{S}''_3 - k|\tilde{S}''_3|)^m \right]$$

$$\tilde{s}' = \begin{bmatrix} s'_{xx} \\ s'_{yy} \\ s'_{zz} \\ s'_{xy} \\ s'_{yz} \\ s'_{zx} \end{bmatrix} = \mathbf{C}' \mathbf{s} = \begin{bmatrix} c'_{11} & c'_{12} & c'_{13} & 0 & 0 & 0 \\ c'_{12} & c'_{22} & c'_{23} & 0 & 0 & 0 \\ c'_{13} & c'_{23} & c'_{33} & 0 & 0 & 0 \\ 0 & 0 & 0 & c'_{44} & 0 & 0 \\ 0 & 0 & 0 & 0 & c'_{55} & 0 \\ 0 & 0 & 0 & 0 & 0 & c'_{66} \end{bmatrix} \begin{bmatrix} s_{xx} \\ s_{yy} \\ s_{zz} \\ s_{yz} \\ s_{zx} \\ s_{xy} \end{bmatrix}$$

[1] Hill, R., 1948. A Theory of the Yielding and Plastic Flow of Anisotropic Metals, 281-297.

[2] Barlat, F., Aretz, H., Yoon, J.W., Karabin, M.E., Brem, J.C., Dick, R.E., 2005. Linear transformation-based anisotropic yield functions. International Journal of Plasticity 21, 1009-1039.

[3] Plunkett, B., Cazacu, O., Barlat, F., 2008. Orthotropic yield criteria for description of the anisotropy in tension and compression of sheet metals. Int J Plasticity 24, 847-866.

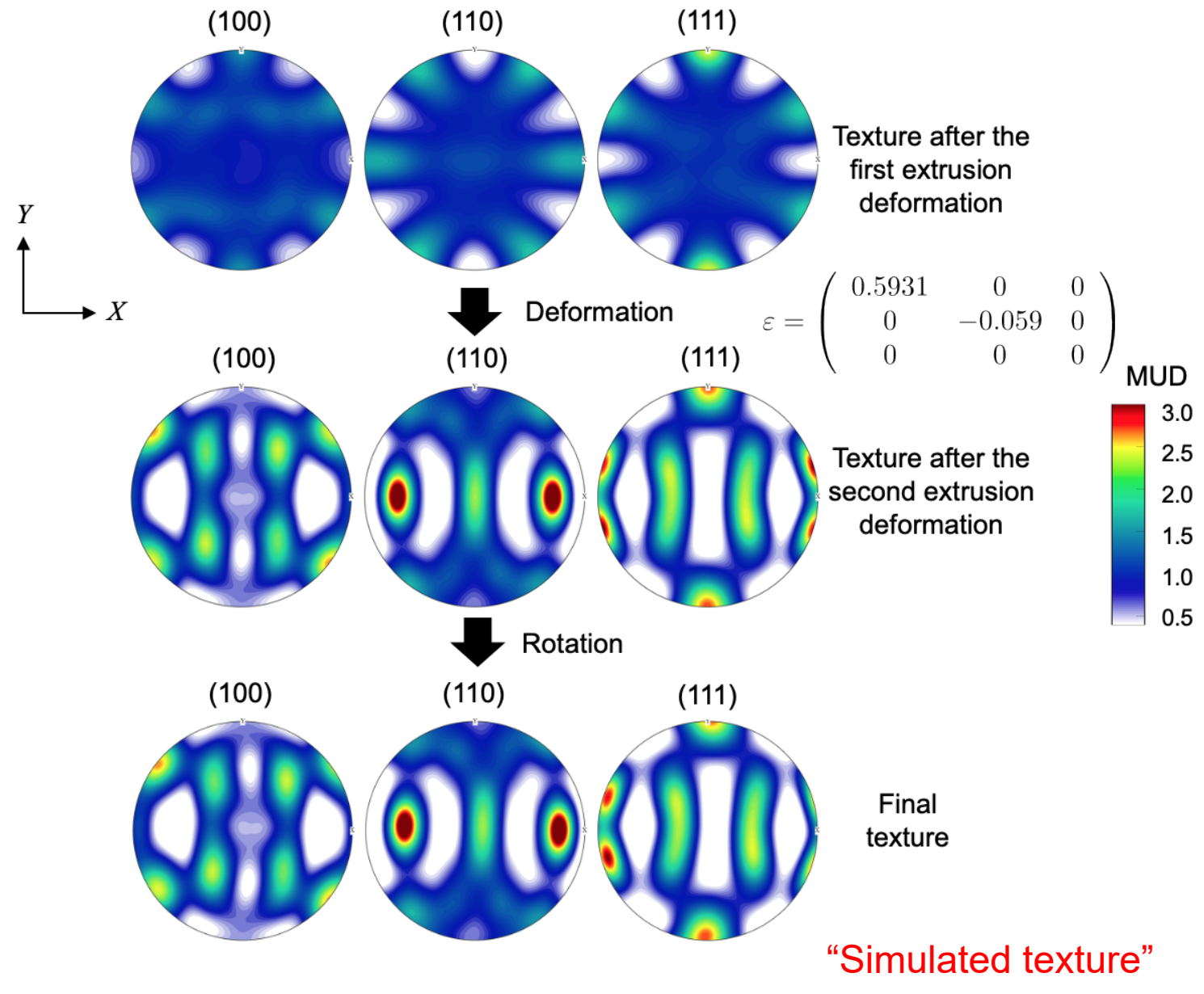
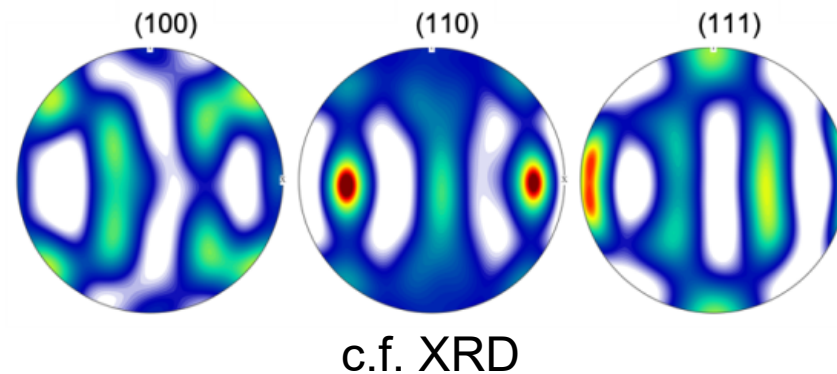
# Computational microstructure 2: Simulated texture



CP-FEM typically assumes uniform dislocation distributions and intragranular crystal orientations



Perform extrusion simulations that reproduces measured texture & heterogeneous intragranular features

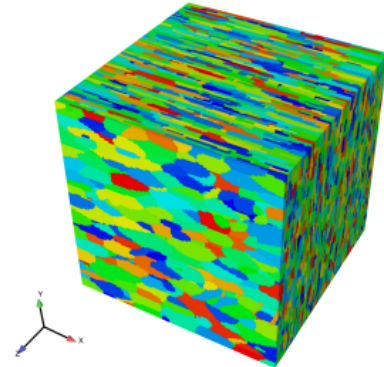


# Outline



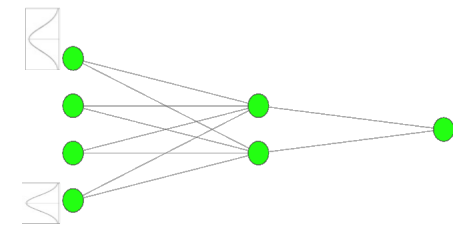
## 1. Predicting plastic anisotropy using large-scale crystal plasticity finite element simulations<sup>1,2</sup>

Investigating the effects of heterogeneous microstructural features and constitutive models on plastic anisotropy predictions using crystal plasticity simulations.



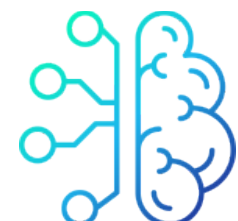
## 2. Predicting plastic anisotropy using Bayesian neural network surrogate models<sup>3,4</sup>

Developing an efficient data-driven protocol to accurately predict plastic anisotropy from initial crystallographic texture using Variational Bayesian Inference techniques



## 3. Revolutionizing Manufacturing through Machine Learning

Revolutionizing the manufacturing process by eliminating the need to perform expensive, timely, and resource heavy mechanical materials test by utilizing the power of machine learning.



# Effects of CP hardening model

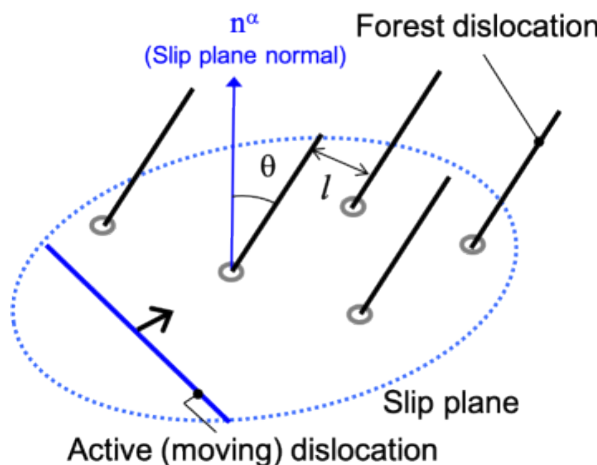


Slip resistance: 
$$g^\alpha = g_0 + A\mu b \sqrt{\sum_{\beta=1}^{12} H^{\alpha\beta} \rho^\beta}$$

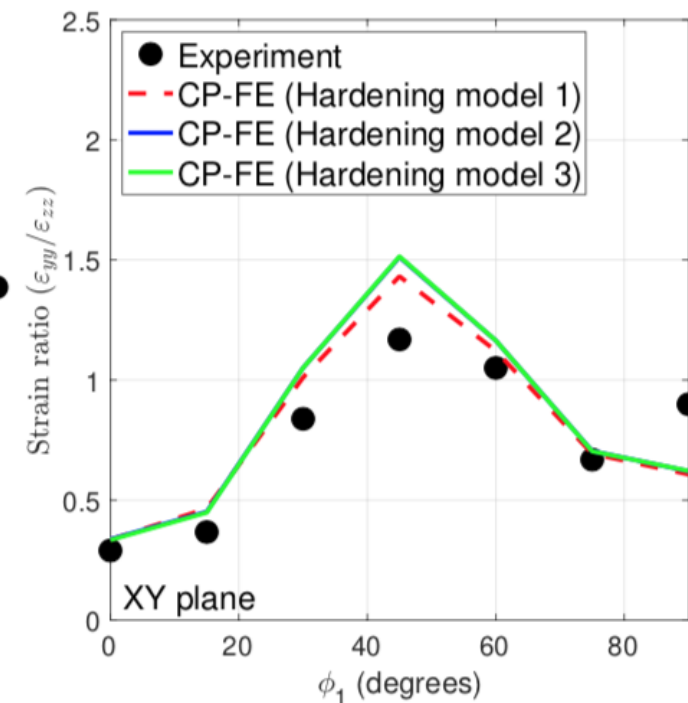
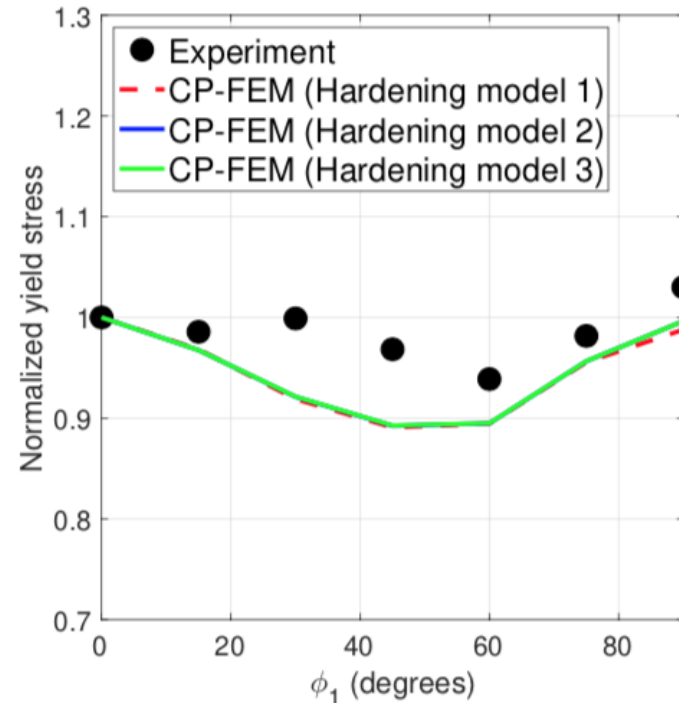
$$H^{\alpha\beta} = 1 \quad (\text{Model 1})$$

$$H^{\alpha\alpha} = 1 \quad H^{\alpha\beta} = 1.4 \quad (\text{Model 2})$$

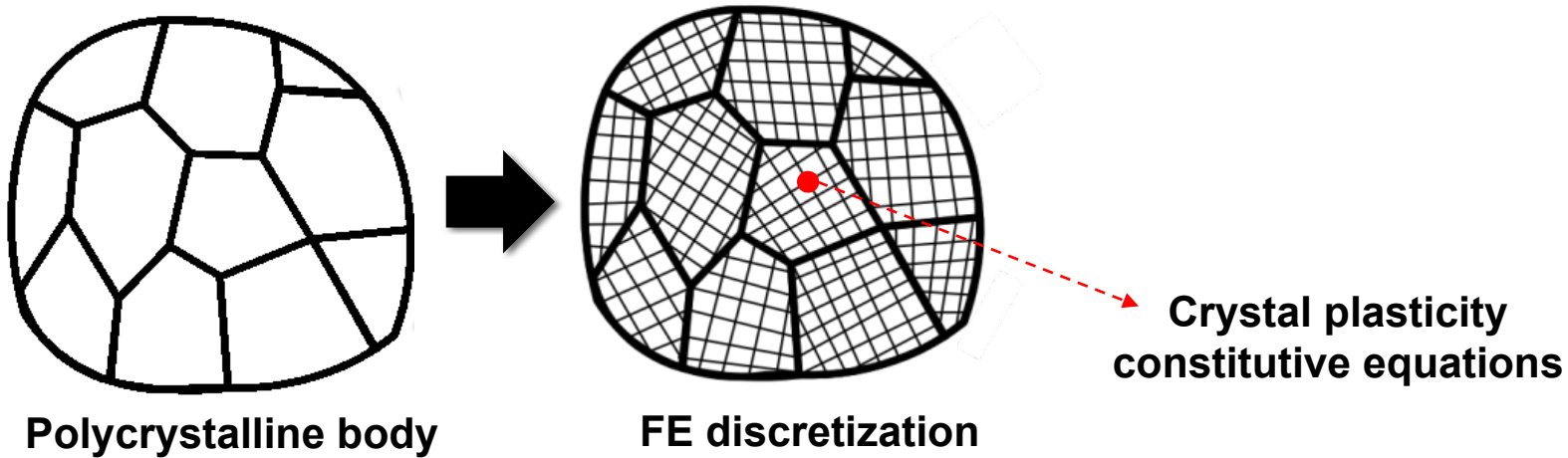
$$H^{\alpha\beta} = \mathbf{n}^\alpha \cdot \boldsymbol{\xi}^\beta \quad (\text{Model 3})$$



Lee et al., IJP (2010)



# Crystal Plasticity – Finite Element (CP-FE) method

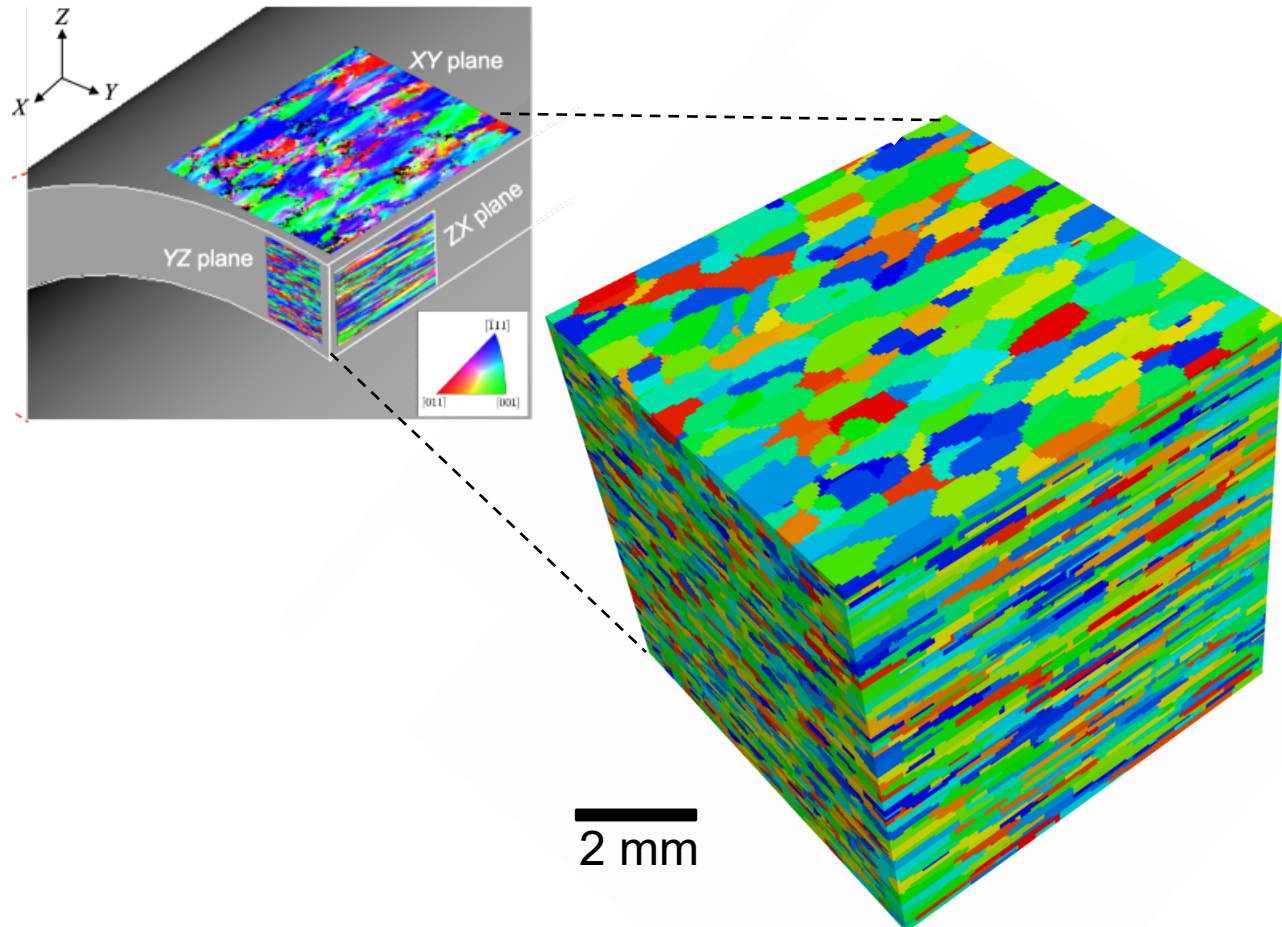


- Grain-level (mesoscale) approach to materials modeling using multiscale strategies – realistic length and time scales
- Explicitly model discrete grains and slip systems based on dislocation slip
- Predicts heterogeneous material's responses resulting from microstructure.
- More predictive than macroscopic plasticity models (e.g. texture evolution and elastic/plastic anisotropy)

- **Slip rate:**  $\dot{\gamma}^\alpha = \dot{\gamma}^0 \left( \frac{\tau^\alpha}{g^\alpha} \right)^{1/m}$
- **Slip resistance:**  $g^\alpha = g_0 + A\mu b \sqrt{\sum_{\beta=1}^{12} H^{\alpha\beta} \rho^\beta}$
- **Dislocation evolution:**

$$d\rho^\alpha = \left( \kappa_1 \sqrt{\sum_{\beta=1}^{12} \rho^\beta} - \kappa_2 \rho^\alpha \right) |d\gamma|$$
- **Hardening matrix:**  $H^{\alpha\beta} = \mathbf{n}^\alpha \cdot \boldsymbol{\xi}^\beta$
- **12  $\{111\}<110>$  slip systems for FCC**

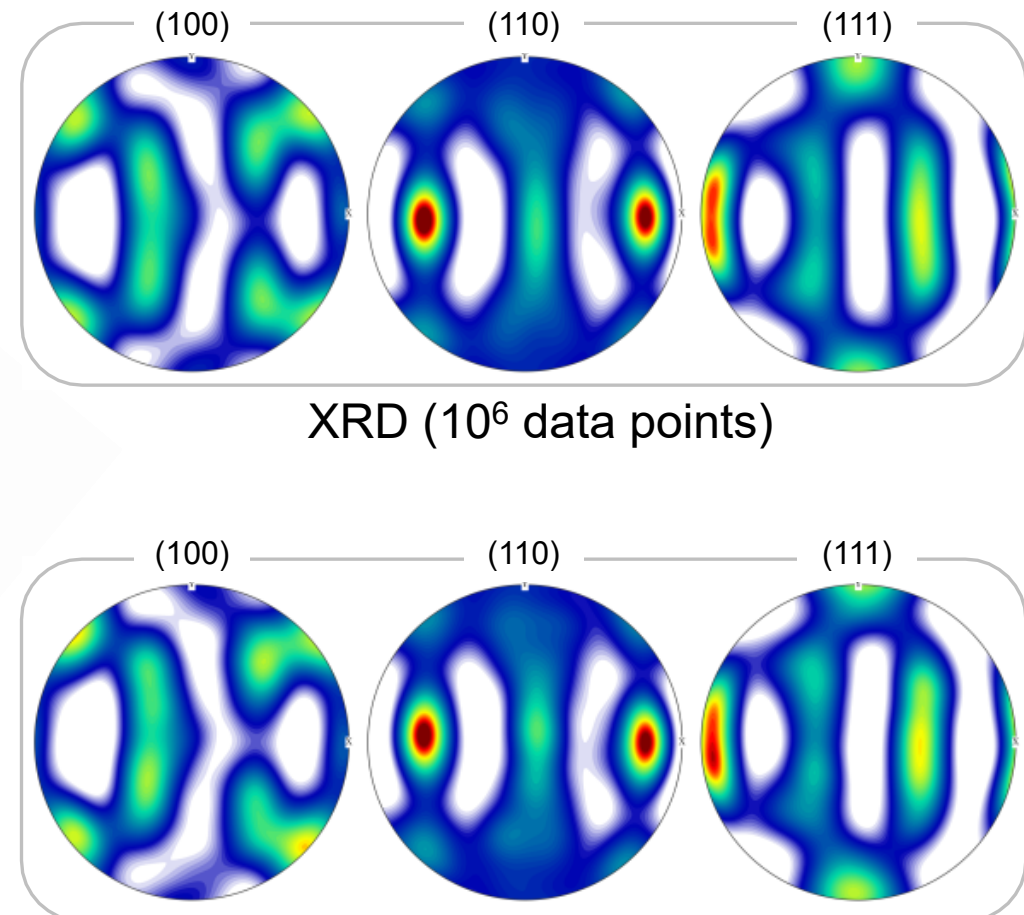
# Computational microstructures 1: Sampled texture



FE mesh: 3,375,000 ( $150 \times 150 \times 150$ ) hex elements

Average grain aspect ratio  $\sim 7:3:1$  along X, Y, Z directions

RVE with  $\sim 3,000$  grains

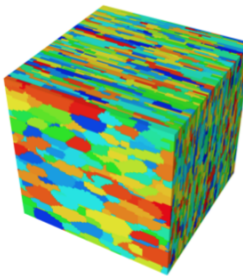
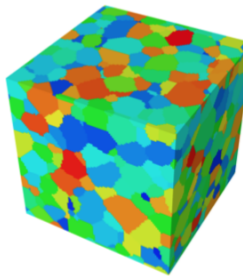
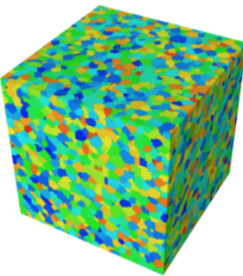
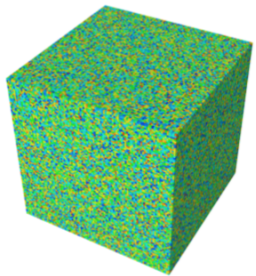


"Sampled texture"

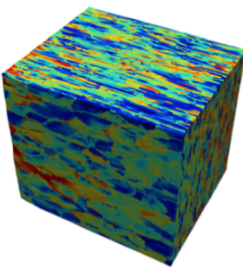
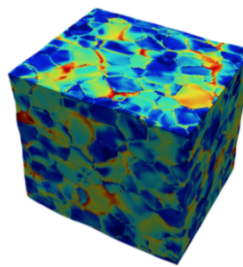
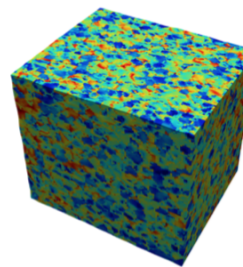
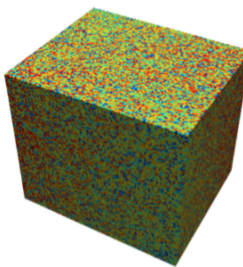
# Effects of initial microstructures



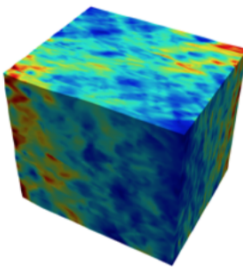
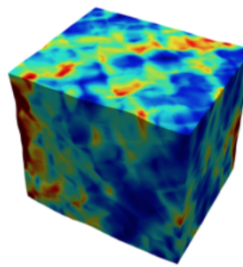
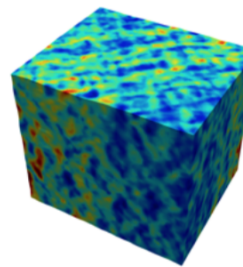
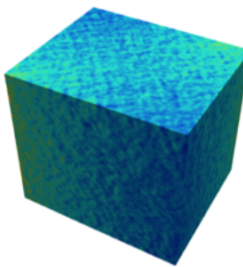
Single element grains    Equiaxed grains (fine)    Equiaxed grains (coarse)    Elongated grains



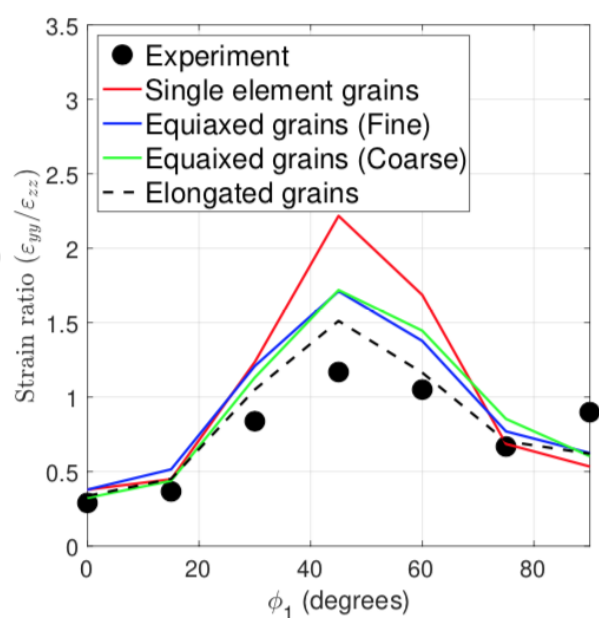
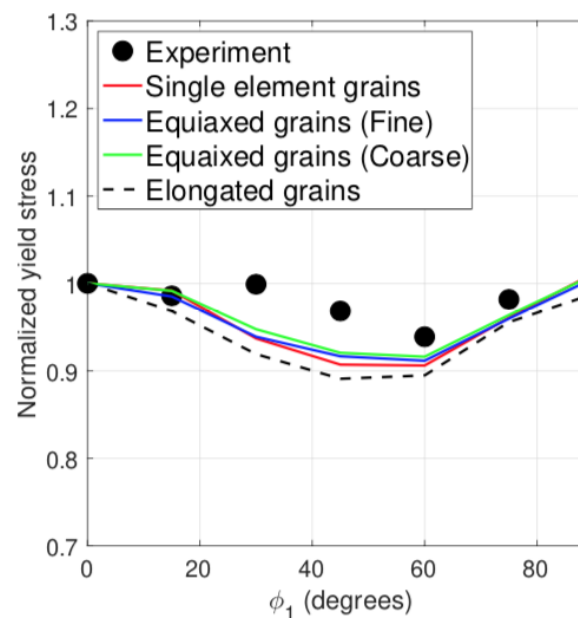
(a) Initial microstructures



(b) Von Mises stress fields (MPa)



(c) Equivalent plastic strain fields



# CP-FE simulations

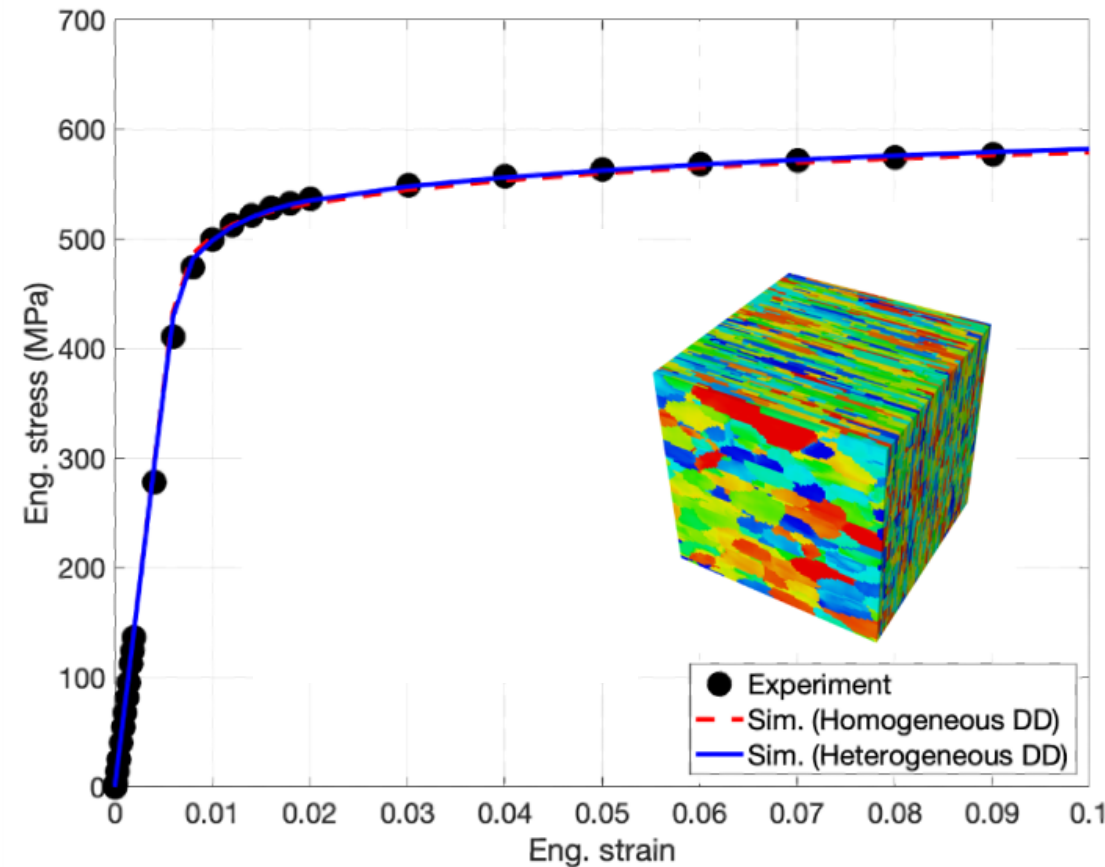
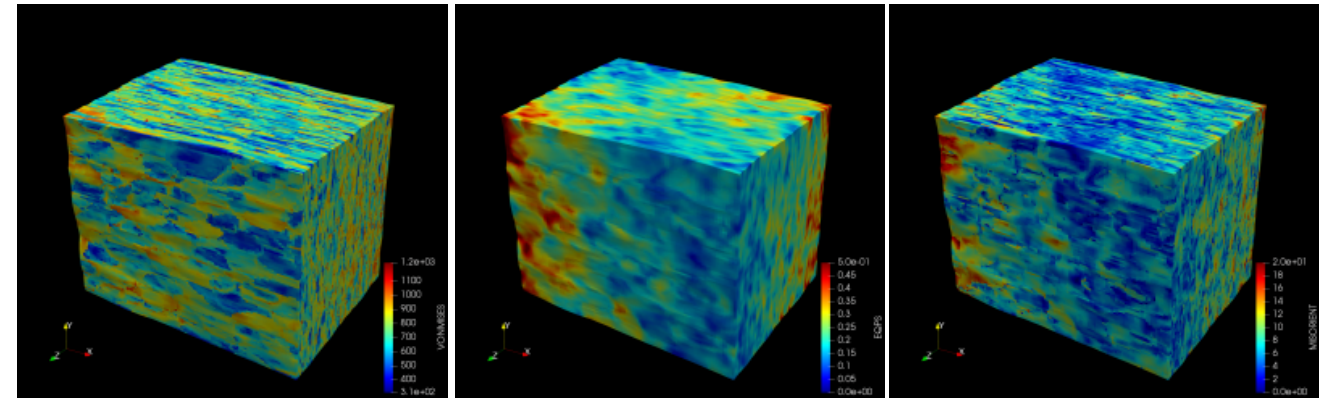
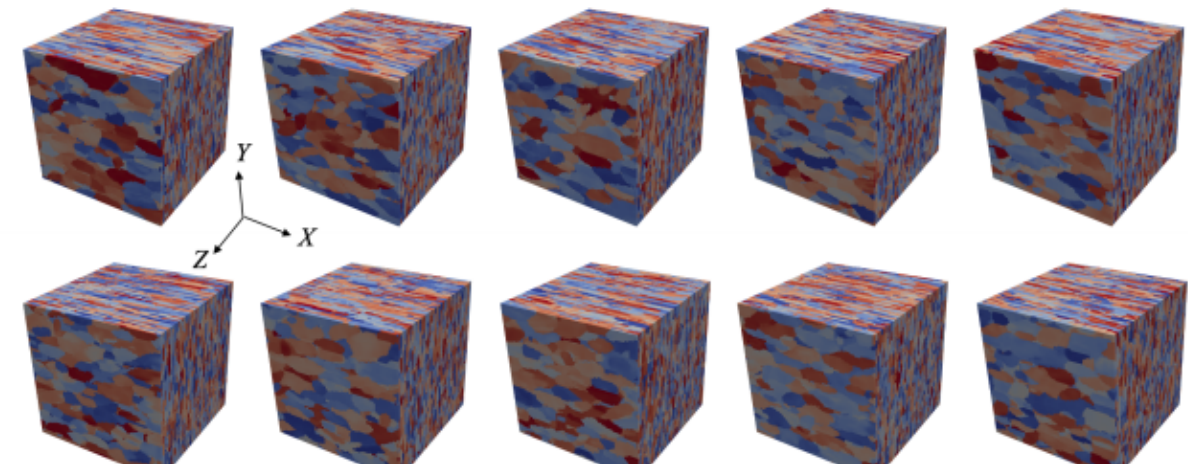


**Table 2.** Material parameters used in the sampled texture CP-FEM simulations.

Constants	Values	Constants	Values	Constants	Values
$C_{11}$	108.2 GPa	$\dot{\gamma}_0$	$10^{-5} \text{ s}^{-1}$	$\rho_0$	$1.17 \times 10^{14} \text{ m}^{-2}$
$C_{12}$	61.3 GPa	$m$	0.012	$\kappa_1$	$4.0 \times 10^8 \text{ m}^{-1}$
$C_{44}$	28.5 GPa	$A$	0.4	$\kappa_2$	28
$\mu$	25.7 GPa	$b$	$2.86 \times 10^{-10} \text{ m}$	$g_0$	143 MPa



*Deformed microstructures at 20%*



*10 realizations of equivalent microstructures*